Gas Embolism: Fundamentals, Diagnosis, and Treatment

Mohammad Mahdi Mardanpour, Dan V. Nicolau Jr., Richard E. Moon, Neal W. Pollock, David M. Eckmann, and Dan V. Nicolau, *Member, IEEE*

(Clinical Application Review)

***Abstract*—Invasive medical interventions or abrupt reductions in ambient pressure can result in intravascular gas embolism. The accumulation of gas bubbles initiates a cascade of pathophysiological phenomena progressing from platelet activation to ischemia and neurological dysfunction. This review integrates current knowledge of the biophysical mechanisms of bubble nucleation, progression, and vascular occlusion into a framework aligned with the adverse physiological consequences on circulation. The discussion further addresses the present state of clinical practice, diagnostic approaches, and therapeutic interventions. Initial studies on gas embolism utilized *in vivo* models, and recent *in vitro* and *in silico* platforms have provided reproducible and cost-efficient experimental approaches. The initial symptoms of gas embolism often overlap with stroke, myocardial infarction, or sepsis. Reliable detection of intravascular gas bubbles is constrained by the sensitivity, resolution, and accessibility of existing imaging modalities, particularly in systemic cases. Current treatment frameworks emphasize hyperbaric oxygen therapy, while adjunct pharmacological strategies to improve clinical outcomes are under investigation. The challenges responsible for the persistent neglect of gas embolism in both clinical and academic contexts are discussed, and a forward-looking perspective on strategies to overcome these barriers is presented.**

***Index Terms*—Gas embolism, decompression sickness, iatrogenesis.**

Manuscript received 20 August 2025; revised 18 November 2025, 24 January 2026, and 20 March 2026; accepted 20 March 2026. This work was supported in part by the U.S. Office of Naval Research under grant N000142512234 and in part by the Natural Sciences and Engineering Research Council of Canada under Grant RGPIN-2022-04053. *(Corresponding author: Dan V. Nicolau.)*

Mohammad Mahdi Mardanpour and Dan V. Nicolau are with McGill University, Montreal, QC H3A 0G4, Canada (e-mail: dan.nicolau@mcgill.ca).

Dan V. Nicolau is with King's College London, WC2R 2LS London, U.K.

Richard E. Moon is with Duke University, Durham, NC 27708 USA.

Neal W. Pollock is with Université Laval, Québec, QC G1V 0A6, Canada.

David M. Eckmann is with The Ohio State University, Columbus, OH 43210 USA.

This article has supplementary downloadable material available at https://doi.org/10.1109/RBME.2026.3677292, provided by the authors.

Digital Object Identifier 10.1109/RBME.2026.3677292

I. Introduction

GAS embolism is a potentially life-threatening condition triggered by gas bubbles entry into the bloodstream. These gas bubbles (emboli) can result from accidental or intentional introduction of gas in blood vessels during medical procedures. Alternatively, gas bubbles can be generated inside blood as the result of considerable and rapid reduction of the surrounding pressure, such as deep-sea diving or high-altitude aviation (Fig. 1(a)). Intravascular bubbles can obstruct the flow of blood and thus impair the transport of oxygen and nutrients to tissues, potentially leading to neurological damage, organ failure, or death, depending on the location and severity of the blockage [1].

At the microscopic level, once gas bubbles are present in the microvasculature, they can expand (if dissolved gas pressure exceeds ambient pressure), coalesce, and become encapsulated with proteins and platelets, initiating a cascade of pathophysiological phenomena leading to clot formation and vascular inflammation [2]. Aside from the intensification of the obstruction of microvasculature, these processes can also initiate secondary thromboembolic complications, further reducing oxygen delivery to critical organs (Fig. 1(b)) [3]. While these processes are known, the full biological consequences of gas embolism remain unclear.

A key challenge to the study of gas embolism is the diversity of contexts in which it arises. For instance, rapid reduction of ambient pressure can promote the genesis of emboli to have 'global' effects, such as in accidental decompression in deep-diving or high-altitude aviation [4], or 'locally', such as during surgical interventions where air may accidentally access the bloodstream through a point of entry [5]. In both cases, gas embolism may remain undetected until symptoms are apparent, such as regional swelling, pain, or dysfunction [6], or following abrupt cardiovascular collapse or severe neurological deficits [7].

Gas embolism can be also classified according to the circulatory system affected: venous- (VGE) [8] and arterial gas embolism (AGE) [9]. VGE is typically associated with surgical accidents, possibly leading to pulmonary complications [10], whereas AGE, commonly, but not exclusively, caused by barotrauma or decompression sickness (DCS), poses a greater risk due to its potential to block critical arteries supplying oxygen and nutrients to the brain, heart, and kidneys [11] (Fig. 1(c)). These classifications can be clinically important, as they affect

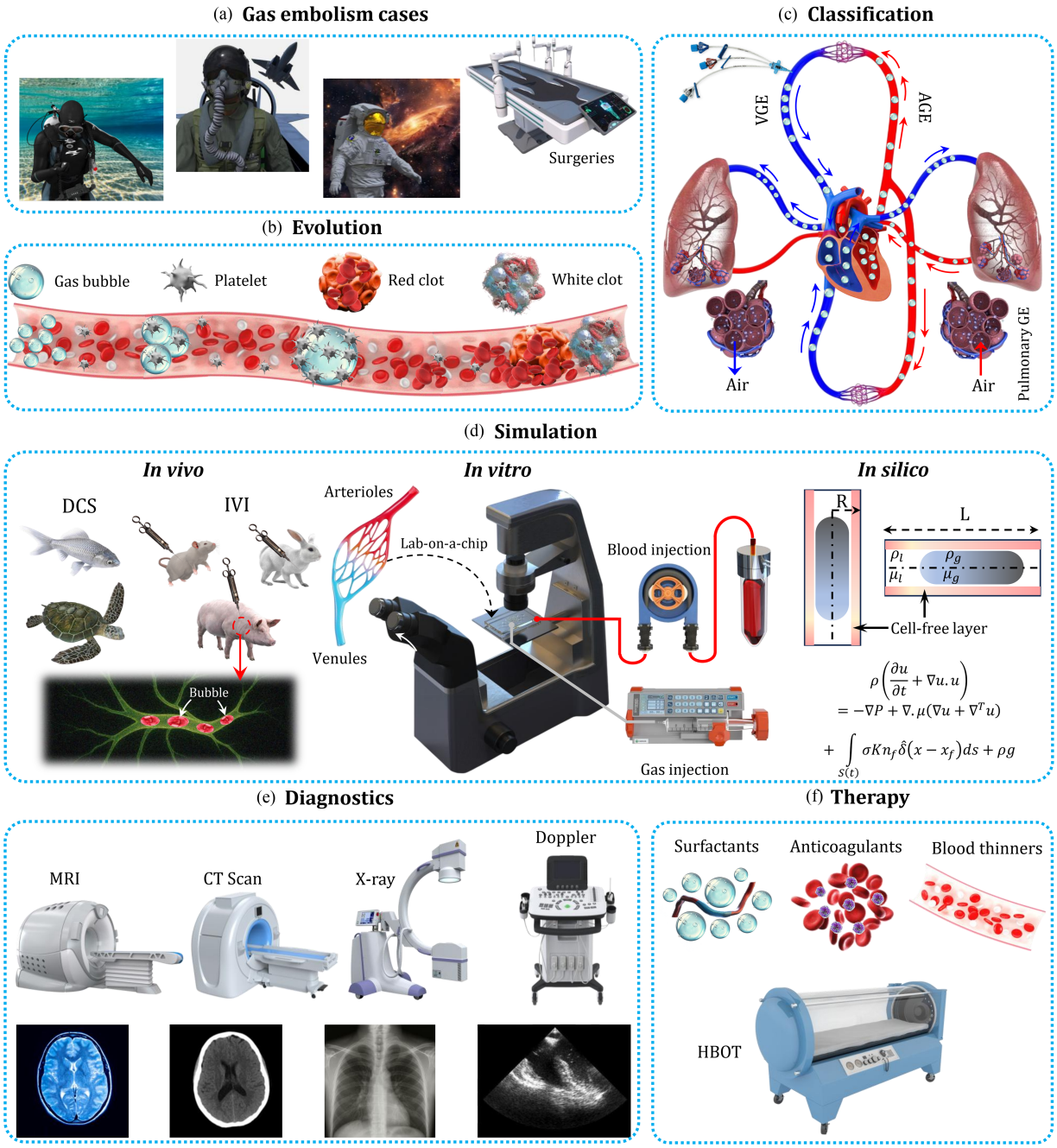

Fig. 1. *Conceptual overview of gas embolism - an integrative roadmap summarizes the major thematic domains of the present review.* (a) Gas embolism cases arising during medical procedures or from extreme environmental exposures such as deep-sea diving or high-altitude aviation. (b) Progression of gas bubbles within microvasculature, including aggregation, expansion, coalescence, encapsulation by platelets, white clot formation, and subsequent red clot development. (c) Classification of gas embolism into arterial gas embolism (AGE) and venous gas embolism (VGE), along with the direction of gas bubble movement within the circulatory system. (d) *In vivo* simulation of gas embolism via intravenous injection (IVI) or exposure to high-pressure water mimicking decompression sickness (DCS); *in vitro* modeling through fabrication of mimicked microvasculature and simulation of iatrogenic gas embolism; and *in silico* modeling through classical fluid dynamics approaches with interfacial forces and non-Newtonian effects included. (e) Current diagnostic approaches for gas embolism, including imaging techniques. (f) Therapeutic strategies such as pharmacological interventions and hyperbaric oxygen therapy (HBOT).

both how the condition presents and how urgently it must be treated.

To advance the understanding of gas embolism, the replication of embolism-like events was implemented in *in vivo*, *in vitro*, and *in silico* platforms. Animal models have been instrumental in advancing understanding of gas embolism pathophysiology. Complementary *in vitro* models and *in silico* simulations can be useful in addressing specific mechanistic questions and facilitating translational research applicable to human physiology [12], [13], [14], [15], [16], [17]. Emerging lab-on-chip platforms mimicking human microvasculature offer a promising *in vitro* alternative [18], [19], [20], [21], [22], [23], due to the capability

of controlling experimentation on the dynamics of gas bubbles under physiologically relevant conditions (Fig. 1(d)). However, presently, due to the novelty of this approach, the integration of the findings of these studies into translational and clinical practice remains limited.

Additional challenges exist related to the diagnosis and management of gas embolism. Early detection is possible, in principle, using medical imaging, e.g., MRI, CT scans, and Doppler ultrasound, but these approaches often lack the resolution or immediacy required [24] (Fig. 1(e)). Additionally, current therapies, mainly hyperbaric oxygen and pharmacological interventions, are inconsistently applied across different embolism types [25] (Fig. 1(f)).

Given the diverse etiology and clinical impact of gas embolism, including iatrogenesis, an urgent need exists for the consolidation of the current knowledge, identification of challenges and future directions of research, and translational medicine. This review discusses the fundamental mechanisms of gas embolism, with emphasis on the dynamics of gas bubbles and cellular responses within the microvasculature, also surveying recent investigations using microfluidic technology to replicate gas embolism events at the microscale. The present state of the art in the diagnostics of gas embolism is then considered, identifying the limitations of the present approaches. Current therapeutic strategies are then reviewed, emphasizing the translational gaps and technological barriers that hinder effective clinical application. By weaving together mechanistic insights, modeling advances, and clinical challenges, this review aims to highlight unresolved questions, inform future research, and contribute to improved detection, treatment, and prevention of gas embolism.

II. Biophysical and Clinical Fundamentals

A. Biophysical and Biochemical Fundamentals

A large and sudden reduction in exposure pressure, whether localized within specific vascular regions or systemically exerted throughout arterial and venous networks, can disturb the equilibrium of dissolved gases in blood, interstitial fluid, and tissues, resulting in the formation of intravascular and extravascular gas bubbles [1]. From a purely biophysical perspective, the governing principle of gas thermodynamics indicate that gas solubility in a liquid medium is directly proportional to its partial pressure [26]. A rapid and substantial drop in ambient pressure causes blood and tissues to become supersaturated with dissolved gases, which if sufficient leads to their transition from the dissolved state into the gas phase, thus initiating bubble nucleation [27]. Among respiratory gases, nitrogen has a lower solubility than oxygen and carbon dioxide [28]. During inadequate decompression, such as that which can occur in deep-sea diving, the bloodstream becomes supersaturated with dissolved inert gas, initiating the nucleation of bubbles within the microvasculature [29]. This phenomenon is the principal mechanism in the pathogenesis of DCS [30].

Gas volume increases proportionally with decreasing ambient pressure, according to Boyle's Law [31]. Consequently, in hypobaric environments, e.g., high-altitude aviation, volumetric expansion can lead to the enlargement of pre-existing gas, which is a factor that causes altitude-related DCS [9]. The development of pulmonary bullae observed after flight exposure exemplifies a physiological effect of expanding gas on pulmonary circulation and risk of AGE [32].

In addition to systemic alternations in gas equilibrium, iatrogenic gas embolism can result from the introduction of gas into the vascular system during medical interventions [6]. Three conditions are required for local gas entry: (i) an external gas source, e.g., atmospheric air or insufflated gas; (ii) a conduit for gas transit, e.g., vascular access devices, surgical tracts, or vessel breaches; and (iii) a pressure gradient driving gas flow into the bloodstream [33]. Many clinical scenarios create environments conducive to these conditions. These include direct insufflation during laparoscopic sleeve gastrectomy [34], high-pressure infusions as in thoracoscopy [35], and negative pressure environments encountered in neurosurgical procedures such as craniotomy [36]. Malfunctions of medical devices, for example, stapler failures in lobectomy [37] and catheter breaches during coronary angiography [38], can alter normal pressure at the site of injury and facilitate iatrogenic vascular gas entry. In the context of iatrogenic gas embolism, VGE predominates over AGE [8], largely because the lower operating pressure of venous system makes it more susceptible to gas entry, especially when central venous pressure (CVP) drops below atmospheric pressure [39].

Beyond pressure-related factors, thermal gradients can also contribute to the initiation of gas embolism. A rapid increase in tissue temperature reduces the solubility of dissolved gases in blood and tissues and can trigger the formation of bubbles. Rapid rewarming of hypothermic patients [13] and the administration of hyperthermic intraperitoneal chemotherapy [40] are clinical examples in which temperature elevation may lead to nucleation of gas bubbles.

The physical properties of gas and blood critically influence the formation, stability, dynamics, and dissolution of gas bubbles [1], [23]. Regarding interfacial properties, small bubbles (radius <50 μm), are particularly affected by surface tension. An increase in surface tension exerts an inward-directed Laplace pressure that elevates the internal gas pressure, facilitating the dissolution of gas bubbles and potentially reducing the risk of gas embolism [1]. From a rheological perspective, an elevation in blood viscosity increases hydrodynamic resistance to bubble motion, which may restrict bubble migration through the microvasculature and simultaneously increase the likelihood of bubble entrapment and microvasculature obstruction [23].

Gas bubbles in the microvasculature initiate a cascade of pathophysiological responses. As illustrated in Fig. 2, bubbles can (a) aggregate or enlarge, forming emboli that obstruct microvasculature [41]. Plasma proteins and platelets (b) adhere to bubble surfaces [42]. Platelet adhesion (c) triggers platelet activation activates additional platelet recruitment and aggregation [43]. This produces platelet-rich thrombi, i.e., white thrombi (d), that intensify microvascular obstruction [44]. The formation of white thrombi triggers secondary coagulation cascades, leading to the formation of fibrin-rich (red) clots (e) [6]. The interactions between bubbles, thrombi, and endothelium cause structural

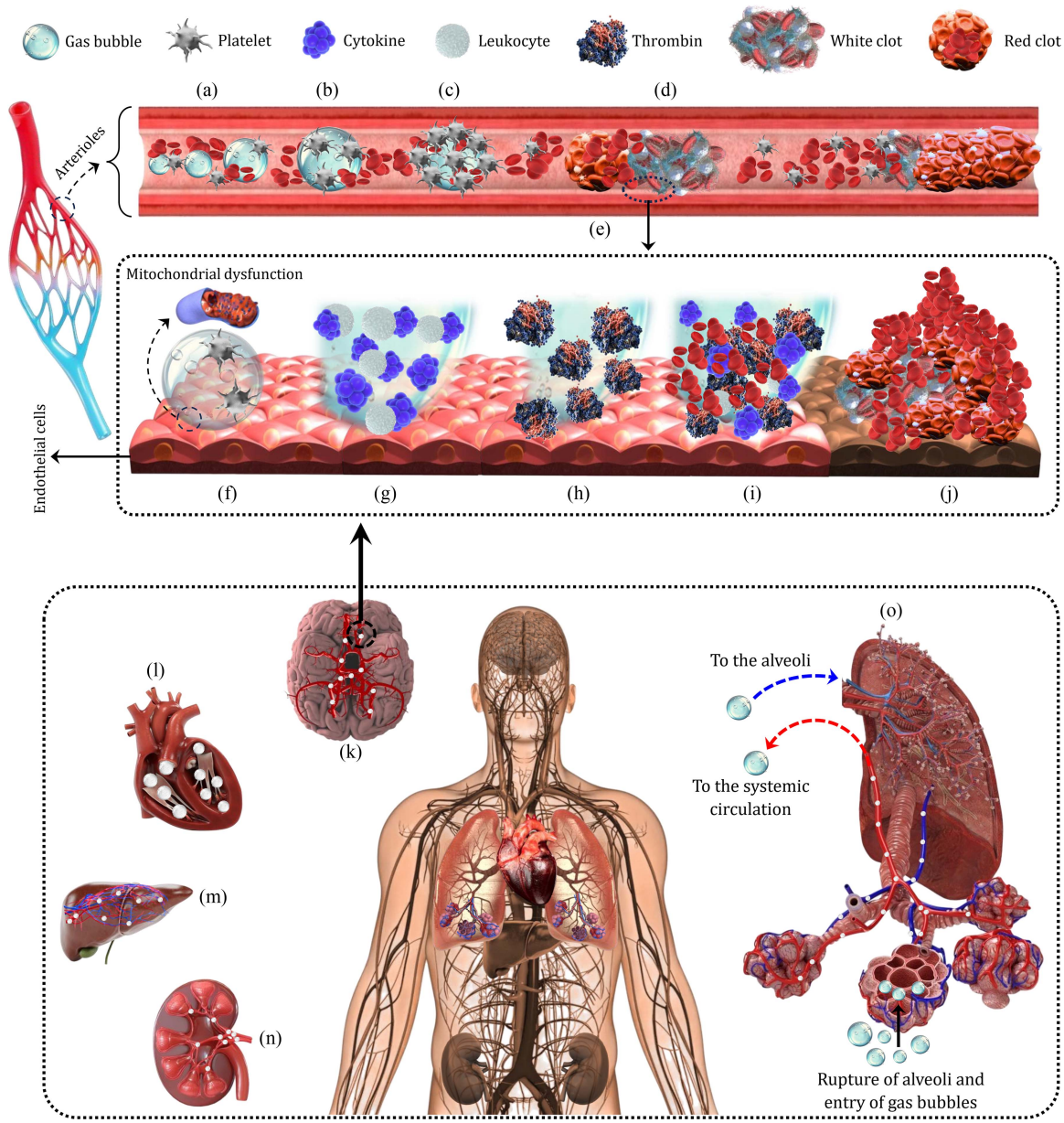

Fig. 2. Gas bubbles entering the systemic or local circulation can lodge within the microvasculature of various organs, obstructing blood flow and leading to localized hypoxia and ischemic injury. The cascade of pathophysiological responses triggered by the presence of intravascular gas bubbles. Events portrayed by individual images (a)–(j) are described in the text. Bottom panel: Typical end organ sites of AGE deposition including (k) brain, (l) heart, (m) liver, (n) kidney, and lung (o) [54].

damage and dysfunction [45], with bubble contact activating a calcium-independent, PKCα-dependent pathway that induces mitochondrial depolarization (f) and endothelial impairment [46]. Endothelial injury triggers a local inflammatory response (g), promoting cytokine release and recruitment of leukocytes [47]. Inflammatory cytokines (TNF-α, IL-1β) upregulate tissue factor, activating coagulation, generating thrombin and fibrin, forming microthrombi (h) that impair perfusion and cause local hypoxia and ischemia [48]. Hypoxia and ischemia impair tissue function, especially in high-oxygen-demand organs such as the brain and heart [49]. Reperfusion after transient ischemia rapidly generates reactive oxygen species and releases pro-inflammatory mediators [50]. Regeneration of inflammatory signaling causes oxidative damage to lipids, proteins, and nucleic acids (i), exacerbating endothelial integrity, vascular injury, clot formation (j), and tissue dysfunction [51]. While many of the signaling pathways and biomolecular processes described here have been demonstrated experimentally in gas embolism or vascular occlusion models, their precise physiological role in the development of clinical gas embolism injury remains incompletely defined. Consequently, several of these mechanisms should be interpreted as biologically plausible contributors to injury rather than fully validated therapeutic targets.

Endothelial and blood cell injury promote the release of microparticles (MPs), submicron vesicles (0.1–1.0 μm) derived from activated or apoptotic platelets, leukocytes, and endothelial cells. Elevated circulating MPs were observed following decompression exposure, suggesting their potential role as early

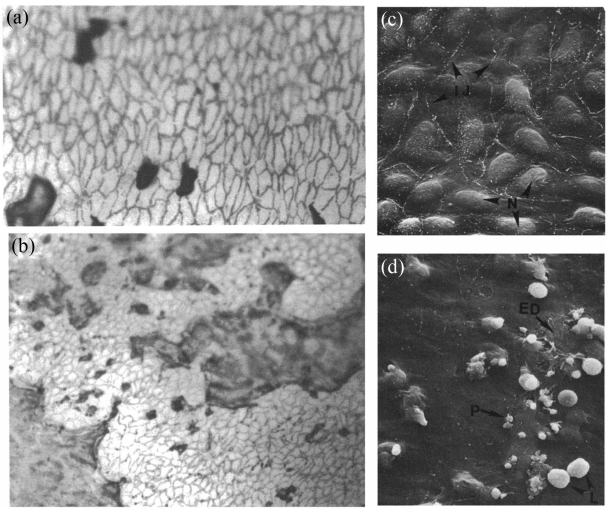

Fig. 3. Endothelial morphology under control and bubble-exposed conditions. (A) Light microscopy of intact porcine pulmonary artery endothelium (control). (B) Pulmonary artery endothelium after exposure to intravascular bubbles induced by compression and decompression in a hyperbaric chamber. Patches of stripped endothelium are visible. (A, B, ×250 magnification, from [57], with permission). (C) Scanning electron micrograph of canine jugular vein (control). (D) Jugular vein after exposure to intravascular bubbles following compression and decompression in a hyperbaric chamber. Endothelial damage is visible. (C, D, ×1000 magnification, from [59], with permission). Abbreviations (black arrows in C, D): IJ-intercellular junction; N-nuclei; P-platelets; L-leukocytes; ED-endothelial damage.

biomarkers of decompression stress, albeit nonspecific ones. These MPs could serve as nucleation sites facilitating bubble growth and act as proinflammatory mediators that amplify neutrophil activation and vascular injury. The accumulation of MPs may contribute to both bubble-induced endothelial activation and downstream inflammatory signaling, enhancing thrombogenic and oxidative pathways [52], [53].

Stripping of the endothelium allows plasma loss into the interstitium causing hypovolemia, hemoconcentration, and sometimes hypovolemic shock [55], [56]. Fibrin, platelets, and activated neutrophils accumulate at the gas-liquid interface. Destruction of endothelium can affect control of vascular tone, resulting in vasoplegia [57], [58]. Leucocytes and platelets adhere to denuded vascular basement membrane [59]. Despite clearance of bubbles from cerebral arteries, local blood flow progressively decreases [60], an effect attenuated by leukocyte depletion [61]. Fig. 3(A)–(D) illustrates endothelial injury in vascular tissues after decompression-induced bubble exposure, and is marked by surface denudation, intercellular disruption, and platelet and leukocyte adhesion.

A more detailed discussion of the interrelated biophysical complexities of blood flow and mass transfer around gas emboli is presented at the beginning of the presentation of *in silico* studies (and Appendix A in supplementary information). A more comprehensive discussion regarding the biochemical inflammatory pathways triggered by gas emboli is presented in Appendix B in supplementary information.

A comprehensive understanding of the biophysical, biochemical and physiological parameters that modulate gas bubble dynamics, including both *in situ* formation of bubbles from dissolved gases during decompression and exogenous entry of gas into the vasculature during medical or barotraumatic events could aid in the development of mechanism-based approaches for preventing and treating gas embolism.

B. Clinical Aspects and Statistical Data

Gas introduction into an artery or vein can occur via several mechanisms, e.g., accidental or intentional air injection during medical procedures, and pulmonary overexpansion causing alveolar rupture during ascent from a scuba dive with breath-holding or due to pulmonary pathology causing gas trapping. This can occur with travel from a depth as shallow as 0.75-1.2 m to the surface [62], [63]. AGE has also occurred during decompression in a dry hyperbaric chamber [64], [65] and in a patient with severe cystic lung disease during depressurization from hyperbaric oxygen therapy (HBOT) [66]. Rarely, focal pathology such as bullae have resulted in AGE during the mild decompression associated with commercial aircraft flight, during which ambient pressure may change from, for example, 1.0 to 0.74 atmospheres absolute (ATA) (sea level to 2438 m; volume expansion of a cystic lung lesion ∼35%). AGE was reported in a man with a large bronchogenic cyst during cable car ascent up a mountain from 1034-3454 m altitude (0.88-0.65 ATA; estimated maximum volume expansion 35%) [67] (see also Table S1-S3, Appendix C, supplementary materials). Interaction of catalase in erythrocytes with hydrogen peroxide can also promote the release of oxygen gas bubbles. Thus, gas embolism can also occur after entry of hydrogen peroxide into the circulation, either by irrigation of a surgical wound or oral ingestion [68], [69].

VGE can occur due to accidental injection of air intravenously, during surgery, where venous or capillary pressure at the surgical site is sub-atmospheric (e.g., craniotomy in the sitting position), or rarely due to an increase in local gas pressure (e.g., pneumoperitoneum during laparoscopic surgery). VGE can also occur during decompression from a scuba dive due to supersaturation of inert gas. VGE is generally filtered efficiently by the pulmonary capillary network. However, VGE can still damage the capillary endothelium [57], [58] and large gas volumes can induce capillary leak and pulmonary edema [70], [71], [72]. Bubbles can traverse the pulmonary capillary network and become AGE with variability determined by species anatomy and physiology [73], [74], [75], especially with cardiac output elevation during exertion [76]. VGE can also bypass the pulmonary filter, and become AGE via right-to-left heart passage through intracardiac structural defects such as atrial septal defects or patent foramen ovale [77].

Although some procedures have been commonly associated with VGE detected using highly sensitive methods such as echocardiography, the incidence of serious cases of AGE during surgery have been reduced due to implementation of several monitoring and preventive techniques. End-tidal PCO_2 ($P_{ET}CO_2$) decreases rapidly in the setting of venous gas embolism, and continuous $P_{ET}CO_2$ monitoring is mandatory for all general anesthetics [78].

While there is substantial incidence of gas embolism in certain neurosurgical and orthopedic procedures, there are no specific clinical guidelines or consensus statements pertaining to

monitoring and prevention outside of those related to craniotomies performed with patients in the sitting position. However, for these procedures the use of precordial Doppler to detect air bubbles is common. In such cases, it is considered prudent clinical practice for gas entry monitoring by transesophageal echocardiography (TEE) or with precordial Doppler ultrasound and for patients to have a central venous catheter inserted into the superior vena cava for possible aspiration of blood and bubbles should air entry be detected. Elimination of air from irrigation fluid during hysteroscopy and elimination from the anesthetic of nitrous oxide, which causes bubbles to increase in size, have also significantly reduced the risk. AGE during cardiopulmonary bypass has been almost completely eliminated due to technical improvements in the oxygenator and routine bubble detection.

Once VGE is suspected, care is predicated on identifying the source of gas entry, prevention of additional gas entry, e.g., clamping or disconnecting tubing, reducing the volume of any gas entrained, and hemodynamic support. Administration of 100% oxygen to reduce bubble nitrogen content should be initiated, and endotracheal intubation should be performed if severe respiratory distress or refractory hypoxemia is present or if the patient is unresponsive. In cases of hemodynamically significant VGE, patients should be positioned to minimize further air entrainment, e.g., head down for air entrainment during sitting craniotomy or from accidentally disconnected central venous catheter. In cases of AGE, it is preferable that patients be placed flat in supine position. The underlying principle for this is that the shear and pressure forces of arterial blood flow propel bubbles downstream until they lodge in the vasculature. This can produce worse cerebral edema in patients who are in a head-down position. In either case, there are no specific clinical guidelines or consensus statements pertaining to central venous pressure management.

Significant variation in statistical data reflects the limited understanding of the occurrence and impact of gas embolism. For instance, DCS reported frequency spans from 0.32 to 35.3 incidents per 10000 person-dives depending on the pattern of diving [79]. The frequency of DCS in diving depends on several factors, such as depth-time profile, decompression procedure, and patterns of thermal state and physical exertion throughout the dive. These parameters can change the probability of DCS by 1-2 orders of magnitude [80]. While iatrogenic gas embolism is also described as rare in clinical practice, e.g., with an estimated incidence of 0.03 cases per 1000 hospitalizations [81], there are reports with substantially higher rates, e.g., with up to 1.3 per 1000 hospitalizations [82]. The reported incidence of iatrogenic gas embolism has also varied widely across procedures, e.g., 0.005% for severe AGE [83]. The incidence of VGE has been reported as 10–50% following hysteroscopy [84], and up to 50% in pediatric laparoscopic appendectomy [85]. Echocardiography can detect subclinical bubbles that often have no ill effect (routine ultrasound monitoring of asymptomatic scuba divers have frequently revealed VGE) [86]. This wide range of statistical data stems in part from the fact that mandatory patient safety and incident reporting is not required in cases of iatrogenic gas embolism (although in some USA states general mandatory reporting mechanisms exist when issues of patient safety occur). Findings can also vary as a function of the sensitivity of monitoring tools, with with the most sensitive detection methods more likely to more cases, many possibly at subclinical levels of gas embolism. The limited understanding of the occurrence and impact of gas embolism is also revealed by the lack of reporting of easy-to-collect medical data (even in the rare published relevant reviews), such as hematocrit concentration, blood pressure, which may be modulators of severe gas embolism [23].

Diagnosis of AGE and initiation of treatment are generally made on the basis of clinical suspicion and neurological exam. Diagnostic tests generally have low sensitivity and the process of obtaining them can delay treatment (Table I). Present medical imaging has a sensitivity that is too low to be clinically useful, and furthermore it could delay definitive treatment. Treatment of AGE is indicated mostly for neurological symptoms or signs, and for pulmonary edema caused by high levels of VGE. Treatment of asymptomatic AGE would be rare, probably only indicated for cerebral bubbles. Imaging should mainly be reserved to rule out other pathologies such as cerbral hemorrhage when there is uncertainly of the diagnosis. Definitive treatment of gas embolism consists of standard supportive care and HBOT. HBOT aims to reduce bubble size (if soon after gas embolism onset) and to accelerate its resolution due to inert gas washout (usually nitrogen), and in addition it provides anti-inflammatory effects [11], [52], [54], [77]. Intravenous lidocaine infusion could reduce secondary inflammation [94]. Repeated hyperbaric treatments may be given until there is no further incremental improvement.

Gas embolism outcomes worsen with delayed therapy, and can result in 33% mortality and 35% incidence of severe neurological effects [91]. While the exact rate of gas embolism during seemingly uneventful exposures remains unknown, studies suggest that such cases may result in significant clinical problems [95]. Reports have described an incidence of VGE as high as 23% [96]. Recent investigations indicate considerable variability in incidence, with gas embolism reported in 10% to 80% of neurosurgical operations and 57% of orthopedic procedures [97]. Surgical procedures such as cesarean deliveries, total hip arthroplasty, craniotomies conducted on patients seated upright, and cardiac operations utilizing cardiopulmonary bypass are also high-risk procedures for gas embolism [3]. A review of 189 published reports revealed that the leading causes of cerebral gas embolism are known to include central venous catheterization (22%), cardiopulmonary bypass (19%), lung biopsy (10%), endoscopic retrograde cholangio-pancreatography, hemodialysis, and mechanical ventilation (each responsible for 6%), and angiography/contrast injection (5%) [5]. Prior clinical events can also affect outcomes. For example, patients with a history of cardiac arrest demonstrated a mortality rate of 54%, in contrast to a 14% rate among those without such events [91]. While clinical studies often follow gas embolism episodes, systematic experimental evaluations remain scarce. Recent experiments involving CO_2 laparoscopy in pigs reported mortality reaching 60%, demonstrating the severity of gas embolism under controlled experimental conditions [98]. In the context of clinical reporting, it is important to note that no large-scale meta-analyses or combinatorial epidemiologic studies of gas embolism occurrence

TABLE I
COMPARISON OF BUBBLE DETECTION MODALITIES

Modality	Sensitivity to gas (*in vivo*)	Spatial resolution	Temporal resolution	Penetration/Target	Clinical accessibility
Precordial Doppler	Very high; can detect individual or clusters of bubbles passing through scanning field	Very low (global cardiac signal)	Discontinuous, real time	Right heart and subclavian vein only	High, very portable but low sensitivity unless bubbles moving through heart [87]. Repeated monitoring is feasible.
TEE	Highest; better sensitivity that TTE	Cardiac chambers & great vessels	Continuous, real time	Heart/Proximal vessels	Moderate (bedside but requires specialist, sedation). Low sensitivity unless bubbles moving through heart [88]. Prolonged monitoring is not feasible.
TTE	Less sensitive than TEE	Cardiac chambers & great vessels	Discontinuous, real time	Heart/Proximal vessels	Moderate, (bedside but requires specialist; sedation not required). Low sensitivity unless bubbles moving through heart [88]. Repeated monitoring is feasible.
TCD	High for cerebral emboli	Artery level (e.g., MCA)	Discontinuous, real time	Cerebral arteries	Moderate, operator dependent. Rarely useful clinically, as it detects emboli in transit but rarely while stationary [89]. Repeated monitoring is feasible.
CT	High if performed early after embolization. Minimum bubble size detectable by CT 0.3-0.5 mm, but not a continuous monitor. Sensitivity <50% [90, 91]	High (vessel/parenchyma)	Single time point	Whole brain/Chest	Readily available for most hospital emergency departments, but has low sensitivity for cerebral AGE and thus low clinical utility. It can be useful for detecting hepatic bubbles, e.g., after hydrogen peroxide ingestion or DCS involving abdominal structures (rare) [92].
MRI	Low for air; high for infarct	Very high	Single time point, slow	Whole brain/Soft tissues	Limited value acutely, best used for diagnostic follow up for brain injury 1-2 days after embolization [91, 93].

Abbreviations: CT-computed tomography; DCS-decompression sickness; TCD-transcranial Doppler; MCA-middle cerebral artery; MRI-magnetic resonance imaging; TEE-transesophageal echocardiography; TTE-transthoracic echocardiography

or outcomes have been performed. Consequently, the literature reports a wide range of estimates reflecting different medical conditions, procedures, detection methods, and reporting practices. Although the literature acknowledges the severity of gas embolism as a key challenge in intensive care units [99], [100], [101], related research and changes to clinical practice remain largely unaddressed.

III. IN VIVO, IN VITRO, AND IN SILICO STUDIES

In vivo studies: Gas embolism was experimentally studied in several *in vivo* systems to understand its pathophysiological origin, bubble dynamics, and -possibly- suggest prevention and therapy guidelines [12], [13], [14], [15], [16], [17]. Early studies focused on determining the threshold for VGE by modulating the rate and volume of gas injection through the localized induction of gas emboli. For instance, experiments of canines demonstrated that slow intravenous infusion (<1 mL·kg^{-1}·min^{-1}) allowed survival after air volumes up to 1377 mL [15]. Cerebral arterial embolism was examined by injecting air into the carotid artery of dogs resulting in 50% mortality at 1–1.25 mL·kg^{-1}, while oxygen yielded 90% survival at 1.5 mL·kg^{-1} [12]. Systemic gas embolism was modeled by exposing goldfish to supersaturated water for defined periods, resulting in features resembling DCS [17]. Although systemic gas embolism was frequently documented in marine turtles [16], fish models provided reproducible and more straightforward experimental alternatives [17]. Studies in rats focused on the influence of thermal gradients on incidence of gas embolism [13] and exploring therapeutic interventions [14].

In vitro studies: While *in vivo* models remain indispensable for developing an understanding of the systemic physiological responses, their inherent limitations in replicating human-specific conditions motivated the development of complementary *in vitro* and microfluidic platforms can provide additional tools for controlled mechanistic investigations.

Microfluidic systems can offer a versatile *in vitro* platform for the study of gas embolism dynamics. These systems have the potential to reveal how interfacial phenomena, vessel mechanics, and hemodynamic conditions may contribute to gas embolism, and facilitate the advancement of predictive models and therapeutic interventions [18], [19], [20], [21], [22], [23]. Polydimethylsiloxane (PDMS) is the material of choice for these microfluidic platforms, offering a combination of elasticity, tunable wettability, gas permeability, and excellent optical properties for microscopic observation [102]. In particular, the oxygen diffusivity and Young's modulus of PDMS resemble those of native blood vessels, supporting its suitability for modelling microvascular biomechanics and transport phenomena. The Young's modulus of PDMS typically ranges between 1.32 and 2.97 MPa [103], which is comparable to reported arterial Young's modulus values ranging from 1.0 to 6.0 MPa with an average of 3.8 $\pm$ 1.7 MPa in the brachial artery and from 1.2 to 7.8 MPa with an average of 4.8 $\pm$ 2.2 MPa in the radial artery [104]. Oxygen plasma treatment was used to modify the inherently hydrophobic surface of PDMS, rendering it hydrophilic and more representative of the luminal surface of blood vessels [105].

Lab-on-chip models focused on investigating the impact of microvasculature architecture, blood rheology, flow dynamics, and clotting tendencies on the occurrence of gas embolism [18], [19], [20], [21], [22], [23]. The flow of sheep blood through a successive bifurcated network (Fig. 4(a)) demonstrated that air bubbles significantly altered the local distribution of hematocrit

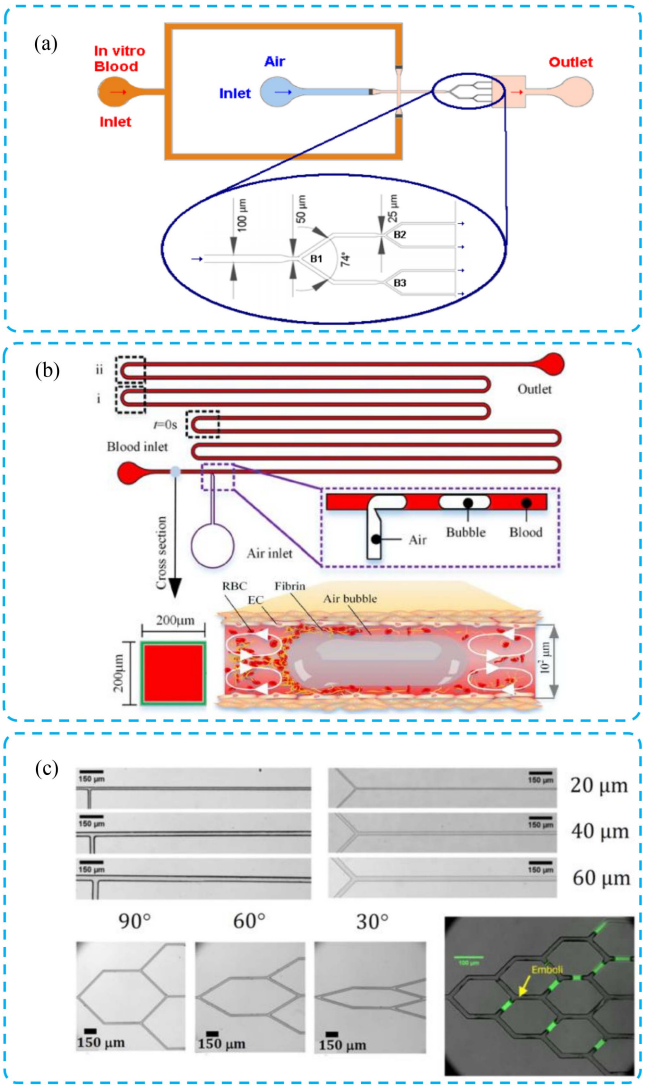

Fig. 4. (a) The architecture of microfluidic network to explore the effect of gas bubble on distribution of local hematocrit. Reproduced from [19] under the terms of CC BY 4.0. (b) The microchannel with square cross-sectional area to reveal the origin and growth of the blood clot at the tail of a bubble at the different positions. Reproduced (layout cropped) from [21] under CC BY-NC-ND 4.0. (c) Partial optical images of the microvasculature structures used for studying the geometrical parameters that modulate gas embolism. Adapted from [23] with permission from the Royal Society of Chemistry.

[19]. This alteration resulted in the upstream accumulation of red blood cells and their depletion downstream of the bubble. The transit of bubbles eliminated the cell-free layer, thus increasing the local shear stress on the vessel walls, which could induce endothelial injury. These findings suggest that bubble dynamics at bifurcations play a key role in microcirculatory disruption and ischemic outcomes associated with gas embolism.

The asymmetric distribution of red blood cells and the influence of vessel geometry were further investigated using alternative microfluidic platforms (Fig. 4(b)) [21]. Air bubbles deformed and gradually come to rest within small vessels due to localized flow fields that promote thrombus formation at the trailing edge of the bubble. As the clot grows, it disrupts the lubrication film between the bubble and the vessel wall, which increases frictional resistance and eventually halts bubble movement. In smaller vessels, the lubrication film is thinner, resulting in earlier contact between the clot and the vessel wall and a higher probability of embolism. Finally, the curvature and the bifurcation impeded the motion of bubbles.

Gas bubble dynamics were investigated in microchannels with T- and Y-junctions and honeycomb networks with varying bifurcation angles (Fig. 4(c)). Gas embolism events were more frequent in T-junctions and honeycomb networks with larger bifurcation angles. Increasing blood viscosity amplified the effect of microvascular geometry. Engineering analysis highlighted the role of forces at the gas–liquid interface, including inertia, pressure, surface tension, and viscosity. The analysis using dimensionless numbers (Weber, Euler, Capillary) can predict embolism onset and identify zones at elevated risk of bubble entrapment [23]. Lower values of these dimensionless numbers indicate an increased risk of embolism. This risk can be mitigated by reducing interfacial tension or increasing bubble velocity, typically achieved by lowering fluid viscosity [23]. For example, lower Weber numbers reflecting reduced inertial forces relative to surface tension, are associated with stronger interfacial effects and a greater likelihood of bubble stabilization and cessation within the microvasculature. Similarly, lower Capillary numbers indicate diminished viscous forces relative to surface tension, which suppresses bubble deformation and splitting and increases the probability of bubble trapping.

Cardiopulmonary bypass investigations demonstrated that microporous membrane oxygenators successfully reduce large gas emboli, but also frequently generate smaller bubbles that may bypass arterial filtration, which highlights the necessity for improved design and bubble-handling strategies [106]. *In vitro* cardiac surgery models employing 3D-printed arterial trees revealed that both the source of entrained air and the cannulation site markedly influence emboli distribution to the brain, with axillary cannulation favoring medium-sized emboli from extracorporeal circuits and aortic cannulation generating larger emboli originating from the heart [107]. At the microscale, microfluidic bifurcation networks replicated microvascular geometry to study bubble lodging behavior, demonstrating that geometry, surface tension, and viscosity determine the stability and movement of trapped bubbles [108].

Advancing toward physiologically relevant models demands developing platforms with 3D configurations designed to reflect the complexity of vascular networks. The inclusion of endothelial cells in engineered microvascular models is also crucial for enhancing biological accuracy and advancing studies on the mechanisms of gas embolism, especially later stages of inflammation and thrombosis. Combined with dimensionless analysis and real-time imaging, these bioinspired models can refine therapeutic strategies and reduce reliance on animal testing, advancing physiologically relevant medical research.

In silico studies: The momentum and mass transfer in moving blood are very complex phenomena, especially at the microscale, because of the overlap and connectivity of the complexities of constitutive elements. Indeed, the liquid-proper part of blood is a non-Newtonian fluid; blood is a multiphasic fluid, consisting

of liquid plasma and 'solid' elements, from the quasi-uniform red blood cells (RBCs) to other particles, which are variable in size and properties, e.g., fat deposits, thrombo-emboli, white blood cells, etc.; all flowing in close contact with the walls of blood vessels, themselves heterogenous in topography, and physico-chemistry [109]. Gas embolism amplifies this already complex system, adding a gas phase, itself consisting of emboli with various sizes and having a membrane modulating the mass transfer towards the liquid phase. To this end, the dynamics of gas embolism are governed by the interplay between surface tension, gas diffusion, and the complex rheological environment of the blood vessels. First, in the vasculature, for a bubble to form, typically by heterogenous nucleation, it must overcome a Gibbs free energy barrier, which is reduced by a factor modulated by the surface tension of the vessel wall [110]. Second, evolution of a bubble size depends on the concentration gradient of dissolved gases between the blood and the bubble surface (described by the Epstein–Plesset equation, modelling diffusion-limited processes) [111]. Additionally, there can be transport of soluble and diffusible material onto, off of, and along the gas-liquid interface, as well as bubble-fluid-wall interactions. In gas embolism, the rapid decompression or exogenous gas entry can result in rapid growth of the bubble, potentially occluding vessels. Finally, in constrained microvascular flow, bubbles lose their sphericity, becoming cylinders with hemispherical caps, with dynamics modulated by the Capillary number, representing the ratio of viscous to surface tension forces [23]. Because blood is non-Newtonian, shear thinning fluid, its effective viscosity decreases as shear rate increases (often modeled by the Casson relationship) [112]. In narrow capillaries, a thin lubricating film of plasma (Bretherton's film) separates the bubble from the endothelium [113]. The pressure drop across such a bubble is significantly higher than in pure liquid flow because the bubble must deform to move, a process resisted by the viscoelasticity of surrounding RBCs (and other 'solid' elements) [21]. A more elaborate discussion is presented in an Appendix (in supplementary materials).

Notwithstanding these complexities, bubble motion and deformation along with interfacial mass transport in blood vessels can be modeled using both computational fluid dynamics (CFD) and analytical techniques, as was begun with the Bretherton bubble problem for a Newtonian fluid [114]. An important consideration in modeling gas embolism is that the radial dimension of the bubble be comparable to the vessel diameter, such that the confining walls influence both the shape and the mobility of the bubble. Calculation of the dynamics of bubble deformation and motion requires that Navier-Stokes equations governing the motion of fluid in both the phases of gas and bulk fluid, i.e., blood, be solved numerically, respecting that large jumps in fluid properties including density and viscosity, as well as high surface tension forces are present. The bulk fluid can be modeled as a two-layer fluid consisting of a cylindrical core of concentrated suspension of RBCs surrounded by a thin cell-free layer near the vessel wall. The cell-free layer is modeled as a Newtonian fluid of constant viscosity, whereas the RBC-containing core layer exhibits non-Newtonian shear-thinning behavior. This can be incorporated through use of a discrete constitutive model for the core viscosity that captures appropriate blood rheology as a function of shear rate. Commonly used models include the Casson, Power-Law, Carreau, Carreau-Yasuda, Walburn-Schneck, and the Generalized Power-law models [115]. The Walburn-Schneck and Power-law models both predict blood rheology very accurately at low, but not high, shear rates. The Casson and the Carreau-Yasuda models capture viscous behavior of blood accurately at low as well as high shear rates. A modified Casson model can also be expressed to account for the specific hematocrit level. The Generalized Power-Law model encompasses the Power-Law model at low shear rates, and the Casson model as a special case for a particular hematocrit level.

There are a number of numerical methods available for solving the governing coupled nonlinear differential equations describing the conservation of mass and momentum that govern the fluid motion, including Volume of Fluid, Level Set, and Arbitrary Lagrangian–Eulerian techniques. While each has its unique strengths and weaknesses, a significant literature addressing gas embolism was published employing an immersed boundary front-tracking scheme coupled with a level contour reconstruction procedure [116], [117], [118], [119], [120], [121], [122], [123]. Results from these studies demonstrate that bubbles in confined Newtonian [116], [117] and non-Newtonian [118], [119], [120], [124] flows generate complex velocity fields, recirculating wakes, and fluctuating shear stresses that govern bubble shape and motion and wall interactions that can mechanically damage the endothelium. Models employing non-Newtonian viscosity laws reveal that the shear-thinning nature of blood significantly affects bubble velocity, residence time, and wall shear stress gradients [117], [118], [119], [120]. Nearly occluding bubbles induce solitary waves of alternating compressive and tensile shear on vessel walls, which can rupture, or activate endothelial cells [116]. This inspires the inclusion of surfactants to alter bubble shape and motion by reducing interfacial mobility and Marangoni effects, as first described by Park [125] for an insoluble surfactant residing on the gas-liquid interface.

Inclusion of transport of soluble surfactants can be incorporated into CFD and analytical models by adding an equation of state for a surface concentration-surface tension relationship, an equation for the evolution of the surfactant concentration at the gas-liquid interface, an equation balancing diffusional flux on the interface with the adsorption/desorption of surfactant between the interface and the bulk fluid, and the convection-diffusion equation governing surfactant transport within the bulk fluid, as outlined in [121], [122]. The modeling must also account for the time-dependent location of the gas-liquid interface [123]. Whether solved via CFD methods or by using analytical asymptotic approaches [118], applications of such mathematical formulations capture the interplay between surface tension, Marangoni stresses, and bubble drag forces, with results showing that both surfactant concentration and yield stress of blood affect bubble behavior: increasing surfactant levels raises drag and slows bubble motion, while non-Newtonian effects modify flow symmetry and shear stress distribution by smoothing out local flow gradients and substantially decreasing harmful shear fluctuations. These findings collectively demonstrate that surfactant-mediated interfacial control can effectively

regulate fluid-structure interactions in gas embolism, offering a mechanistic and quantitative foundation for surfactant-based prophylaxis in clinical settings Additional effects of surfactants as a therapeutic approach are discussed further.

III. Diagnostics

A. Clinical Signs

Symptoms and signs of AGE usually develop within minutes after gas entry, but in some cases may be delayed for more than an hour [126], [127]. Cerebral neurological deficits including confusion, change in consciousness, seizures and focal neurological abnormalities are common [11], [52], [128]. AGE occurring in divers after significant inert gas uptake can present as DCS with spinal cord manifestations [129]. VGE can cause hypotension, respiratory distress, pulmonary edema or cardiac arrest. After initial resolution of symptoms due to treatment, manifestations can sometimes recur [130].

Diagnosis of AGE should rely on clinical history, e.g., rapid ascent, lung pathology, medical or surgical events, and symptoms/signs. In divers, the presence of pulmonary barotrauma including pneumomediastinum or pneumothorax can support the diagnosis of AGE, but is frequently absent. In patients with AGE, brain computed tomography (CT) often shows no bubbles despite severe symptoms [90], [91], and is not recommended to exclude AGE. CT perfusion studies may be a more sensitive and useful diagnostic tool [131]. If there is uncertainty about the diagnosis of AGE imaging is indicated to exclude conditions such as intracranial hemorrhage.

B. Imaging Modalities for Gas Embolism

A variety of imaging approaches have value in the diagnosis of gas embolism. TEE provides the most sensitive means of detecting the presence of gas embolism bubbles within the heart chambers and the pulmonary artery [132]. The utility of TEE is limited to use in sedated or anesthetized individuals, but it can detect as little as 0.02 $mL{\cdot}kg^{-1}$ of gas. While almost all imaging of intravascular gas embolisms occurs *post facto*, real time monitoring of embolism occurrence with this technology typically is observed only in certain neurosurgical procedures such as sitting craniotomies, but it is useful in patients who are hemodynamically unstable where there is a high index of suspicion for gas embolism to have occurred [97].

Radiological techniques are also used to investigate cases of suspected gas embolism. This is particularly challenging given the potentially large number of deposition sites where the gas may ultimately terminate, i.e., the distribution of gas bubbles as convected by blood flow through the vasculature is highly variable. Obtaining imaging studies in gas embolism patients is challenging due to the typical need for extensive resuscitation and stabilization before a definitive diagnosis can be made [133]. Extensive cerebral infarction, often in a so-called watershed distribution of the central nervous system [134], may be the only change to appear on diagnostic studies. Chest radiographs are usually normal, except in cases involving large gas embolus load, in which case areas of hyperlucency may be found overlying the heart shadow, main pulmonary artery, or hepatic veins [3]. Focal pulmonary oligemia, pulmonary edema, or enlargement of the central pulmonary arteries or superior vena cava may be present in such instances [3].

CT scanning is the primary modality for gas embolism diagnosis, as it can demonstrate the above-mentioned features in greater imaging detail. In addition, CT allows the direct visualization and discrimination of gas in systemic venous circulation (typically along the injection trajectory, e.g., subclavian vein, innominate vein, or superior vena cava) as opposed to the right-sided cardiac chambers or main pulmonary arteries, in which gas appears in positive contrast [135]. CT is only diagnostic in the acute setting, since gas is absorbed over time, and the use of lung windows may aid detection [135].

Finally, magnetic resonance imaging (MRI) can be used to evaluate the complications of cerebral gas embolism, i.e., infarction, rather than to detect the presence of bubbles directly. Since gases have very low magnetic susceptibility, they induce significant signal loss on MRI, particularly in gradient-echo mode [136]. However, smaller intracranial air emboli can also be mistaken for blood products or cortical vessels [136].

III. Therapy

A. Initial Treatment

Immediate management of patients with AGE includes standard first aid care, including airway protection, support of blood pressure, and administration of high-concentration oxygen (as close to 100% as feasible). Tissue injury is worsened by hypotension, which should be treated. While mild AGE may not require aggressive initial fluid resuscitation, severe injury with associated hypotension and plasma loss requires aggressive fluid administration to restore intravascular volume. In general, patients with gas embolism should be placed supine, since there is little evidence that buoyancy affects bubble distribution in arterial blood flow, and head-down positioning may exacerbate cerebral edema [11]. Lateral decubitus position is recommended for unconscious patients to minimize the risk of aspiration should a semi-conscious patient regurgitate stomach contents. Massive VGE loads can occasionally be treated initially by aspirating gas from the right heart via a central venous catheter [137]. Based on animal studies, it was proposed that for large volumes of VGE with hypotension placement of the patient into a partial left lateral position (‘Durant maneuver’) may relieve a possible air lock in the right heart and facilitate resumption of blood flow [137], [138].

B. Hyperbaric Oxygen Therapy (HBOT)

The definitive treatment for AGE and DCS is HBOT. A pressure-related reduction of vascular bubble volume is possible if HBOT is initiated rapidly. The use of 100% oxygen creates a high partial pressure gradient for diffusion of inert gas out of bubbles. HBOT also has anti-inflammatory effects that help to mitigate endothelial injury and inflammation. This effect is supported by the clinical observation that in cases where there is incomplete resolution from an initial HBOT treatment

(when complete bubble resolution would be expected), repetitive HBOT usually results in incremental improvement. Early HBOT correlates with better outcomes, particularly in serious cases [139], [140], although benefit may occur, usually in mild cases, even if therapy is delayed up to several days. Other variables that may affect outcome include distribution of bubbles, patient age, and concomitant morbidities such as diabetes, cerebrovascular disease, and cerebral degenerative conditions. Prior to HBOT, chest imaging is recommended to identify pneumothorax, which may require chest tube placement.

Historically, high initial treatment pressures were recommended for AGE treatment: 4-6 ATA with air or mixtures of nitrogen-oxygen or helium-oxygen. However, neither animal studies [141], [142] nor human case series [143] support their superiority over lower treatment pressures breathing 100% oxygen that involve less risk. Treatment protocols such as COMEX-30 (4 ATA) and USN Treatment Table 6A (6 ATA), were also not shown to be superior to treatment at 2.8 ATA for major bubble disease, i.e., DCS [143], [144], [145]. The US Navy Treatment Table 6 [146] is commonly used, employing a 2.8 ATA initial treatment pressure, with compression on air and then a switch to oxygen breathing with air breaks to reduce the likelihood of oxygen toxicity developing. The basic form is a 285 minute treatment. If the patient has not fully responded additional time ('extensions') can be added. Repetitive treatments are recommended on a daily or twice daily basis until a therapeutic plateau is reached, usually within 1-2 sessions [11].

The risks of HBOT include barotrauma, oxygen toxicity, and confinement issues. Middle ear barotrauma is the most common problem associated with both diving and HBOT [147], which is usually managed easily with no long-term sequelae. The incidence of oxygen toxicity seizures during HBOT can be on the order of 0.04% for all treatments [148], or 0.4% for patients treated for decompression illness [149] who typically receive the highest partial pressures of oxygen. Because HBOT involves the use of high concentrations of oxygen under elevated pressure, it poses a fire hazard. Strict operational safety protocols and facility-specific fire prevention measures must be followed, and well-established safety measures have ensured the safe operation of HBOT facilities worldwide [150].

C. Adjunctive Therapy

Adjunctive treatments may include the following:

First air oxygen. Oxygen should be immediately administered, ideally 100% concentration, via mask or, if required, endotracheal tube. This facilitates the elimination of inert gases and promotes hyper-oxygenation of tissues. Oxygen administration at 1 ATA accelerates inert gas elinination from the tissues, and increases venous (and hence tissue) PO_2 modestly [151], [152]. The partial pressure nitrogen gradient from an air pocket or bubble to capillary blood increases from close to zero breathing air to 560 mmHg. The resulting greater rate of diffusion of nitrogen into blood was used to administer oxygen to accelerate the resolution of spontaneous pneumothorax [153]. The promotion of inert gas elimination is a fraction of what is achieved with HBOT, but still very meaningful.

Lidocaine. Adjunctive pharmacologic therapies such as intravenous lidocaine were explored based on experimental evidence suggesting neuroprotective or anti-inflammatory effects, but clinical evidence supporting their routine use remains limited [94]. In animal models intravenous lidocaine improves outcome after AGE, even when HBOT is administered [94], most likely due to its effects on leukocyte adhesion to endothelium and anti-inflammatory effects [154]. Implementation requires a loading dose and infusion (typical loading dose 1.5 $mg \cdot kg^{-1}$ and 24-48 hour infusion at 1 $mg \cdot kg^{-1} \cdot h^{-1}$) to maintain plasma lidocaine levels in the range of 1.5-3 $\mu g \cdot mL^{-1}$. The optimal duration of lidocaine therapy in this setting is not known, however a continuous infusion for 24-48 hours was suggested.

Intravenous fluids. If there is significant hypovolemia caused by plasma leak, fluid resuscitation is recommended to reverse the plasma volume loss. Preferred fluids are isotonic electrolyte solutions that do not contain glucose due to adverse effects of hyperglycemia in brain injury [155].

Anticoagulation. Animal studies suggested that anticoagulation with heparin [156] inhibition of platelet function with clopidogrel [157] might improve outcome, however human data are lacking.

D. Impact of Surfactants on Gas Embolism Events

Gas emboli cause physiological consequences through biomolecular interactions that occur at the gas-liquid interface, including binding interactions with endothelial cells, and initiation of blood clotting and inflammatory pathways [158], [159]. One fundamental approach to reducing the activation such responses is to render the gas-liquid interface biologically inert through introduction of exogenous surfactants, which can outcompete blood-borne macromolecules for interfacial occupancy. Surfactant adsorption-desorption characteristics influence bubble dynamics [160] as well as interfacial shape [161], resulting in modified mechanical and molecular effects of intravascular gas emboli. Interest in surfactants in the therapy of intravascular gas embolism has a long history dating to the early methods of open heart surgery [162]. Modern knowledge of molecular mechanics and molecular biology have opened new avenues for continued pursuit of surfactant-based therapeutics.

In *in vitro* studies of surfactant effects on gas embolism-induced blood clotting, the presence of a surfactant has resulted in up to 70% reduction in thrombin production [163]. Surfactants also reduce platelet activation initiated by bubbles, lowering platelet-bubble and platelet-platelet binding induced by gas emboli [164]. These surfactant effects are dose-dependent and saturable [165]. Accompanying validated Monte Carlo simulations predicted that the surfactants inhibited maximal platelet aggregation by up to 30% [164]. Commonly used surfactants include Pluronic F-68 [166], Pluronic F-127 [163], egg yolk-phospholipids [167], proxanol 268 [118], potassium oleate [168], safflower oil [169], and human serum [170]. Pluronic F-68 and F-127 are effective surfactants approved by the Food and Drug Administration (FDA) for pharmaceutical applications [171], and its ability to reduce the interfacial tension of gas-liquid bubbles is superior to that of other surfactants [163]. These

findings demonstrate that surfactants disrupt the aggregation of emboli and the thrombogenic consequences of gas embolism.

Surfactants may also disrupt the adverse effects of gas emboli on endothelial cell mechanosensing function, which can eliminate the ability of endothelial cells (EC) regulatory inputs to modulate vascular tone. Microbubble contact with endothelial cells induces transmembrane signaling mechanisms, producing calcium entry into cells followed by cell death [172]. The presence of the surfactant reduced the lethality of bubble contact by over 75%. The calcium influx is mediated by a stretch-activated channel that is subjected to mechanical forces coupling the gas-liquid interface and the cell membrane to produce the response [173]. The membrane stretch resulting from bubble/cell mechanical coupling also activates an intracellular signaling pathway that depolarizes mitochondria within cells, leading additionally to endothelial cell bioenergetic dysfunction [46], [174]. The specific biomechanical interactions between the cell and bubble surfaces directly involve macromolecules resident in the endothelial surface layer (ESL), with hyaluran contributing to cell-bubble adherence and heparan sulfate contributing to the calcium transients [175]. Importantly, bubble-induced calcium transients were abolished in the presence of a surfactant. This demonstrates that surfactant adsorption to the bubble surface prevented mechanosensing ESL components from interacting with the gas/liquid interface [176]. These experiments have shown that mechanosensing and stretch-activated channels in the EC membrane couple with the extracellular signal generated by bubble surface interactions to produce the calcium response and loss of mitochondrial potential. These harmful responses are prevented by the presence of surfactants.

Bubble adhesion to the endothelial surface results in obstruction of blood flow. This adhesion results from adsorption onto the bubble surface of macromolecules which are tethered the endothelial cell surface. When the tethering forces exceed the blood pressure forces acting on the bubble, its motion stops [177]. Yet, with a surfactant present in the perfusing medium prior to introduction of the embolism bubble, the adhesion force is reduced and adherence is prevented [177]. Effects of surfactants on bubble interfacial shape and dynamics also accelerate microvascular gas embolization clearance from the vasculature [178]. Bubbles having smaller volume embolized smaller diameter arteriolar vessels if a surfactant were present, with the time to bubble clearance and restoration of blood flow also being decreased. This finding was extended to functional outcomes in *in vivo* cerebrovascular gas embolization [179]. MRI results showed significantly smaller stroke volumes and cognitive and behavioral performance testing showed markedly reduced post-embolic deficits in rats undergoing cerebral AGE when a surfactant was administered intravenously in advance of embolization. These studies effectively demonstrate that surfactants reduce, or eliminate the obstruction of blood flow caused by gas emboli.

Even without adhering to the endothelial surface, passage of a bubble through the vasculature can promote endothelial cell membrane stretch, mechanosensing, and even cell death. Careful multiphase fluid dynamics modeling of bubble motion in a blood vessel has demonstrated the appearance of time variation of shear stress along the vessel wall due to bubble movement [119], [120], [180]. The local blood flow pattern that develops due to the presence of a bubble was verified *in vivo* [21]. This flow field exerts important spatial and temporal effects on the distribution of the shear stress and its gradients along the luminal endothelial cell surfaces. The resultant phenomenon involves initial compression of the local cell membrane, followed by very rapid large-scale stretch and swift recompression. These gradients are further amplified as the bubble dimension tends to full cross-sectional occlusion of the vessel [116]. There are multiple potential physiologic implications of this shear stress wave progressing across the cell surface, including induction of endothelial cell membrane stretch, activation of mechanotransduction pathways, loss of cell membrane integrity, and even cell membrane stress failure. The biological consequences of these on calcium signaling, mitochondrial bioenergetic failure and cell death that can follow were previously described. By tracking the location of the deformable gas-liquid interface [123] and then accounting for a surfactant being transported out of the bloodstream onto the interface [122], it was shown that the magnitude of the shear stress gradients became markedly smaller compared to an equivalent surfactant-free system. Overall, these modeling approaches couple with the body of experimental work to magnify the utility of surfactants as a therapeutic means of reducing the injury potential of intravascular gas emboli.

IV. Perspectives

Despite the potential for health and life-threatening consequences, gas embolism appears to be a relatively overlooked medical condition. Although gas embolism is classical for diving medicine [54] and in certain surgical contexts [6], it is often classified as a complication rather than a distinct disease entity [181]. While this relative lack of interest in gas embolism is partially justified by its *reported* rare occurrence, it also has more fundamental elements, summarized below.

A. Barriers to Prevention, Diagnosis, and Treatment of Gas Embolism

Insufficient surveillance infrastructure: Reliable epidemiological data on gas embolism incidence are virtually nonexistent or insufficient [99]. The lack of convenient measuring capabilities and standardized diagnostic frameworks and frequent confusion with other critical conditions undermine accurate case documentation [8]. As a result, quantifying its true incidence, morbidity, and mortality is challenging [24]. This absence of robust data adversely affects its prioritization in health systems, preventing gas embolism from meeting criteria needed to attract policy initiatives, funding, and infrastructure investment.

Low awareness and sociological barriers: Outside of hyperbaric medicine, e.g., for diving accidents, and specific surgical fields with higher recognized incidence, e.g., cardiothoracic contexts, many clinicians lack training to identify gas embolism. As a result, gas embolism may be misdiagnosed as stroke [182], myocardial infarction [183], or sepsis [184]. Sociological and structural obstacles further intensify these challenges. Although organizations like the Undersea and Hyperbaric Medical Society

(UHMS) [185], Diving Medical Advisory Committee (DMAC), and Divers Alert Network (DAN) [186] address gas embolism in diving and hyperbaric settings, no unified advocacy organization currently exists for the broader patients community [6], [54]. Additionally, from the patient's perspective, gas embolism can lead to long-term complications such as cognitive deficits, chronic pain, and psychiatric conditions, all of which remains poorly documented and often neglected in clinical follow-up and research [187]. Moreover, its occurrence in stigmatized settings, such as unregulated cosmetic procedures [188], illicit drug consumption [189], or medical errors [190], often suppress patient disclosure and result in clinical underdiagnosis. This stigma, in combination with care fragmentation, undermines reliable data collection, restrict translational research, and marginalizes gas embolism in healthcare systems.

Incomplete understanding of fundamental mechanisms: While the pathways of gas entry into the bloodstream through decompression events, trauma, or direct injection during medical interventions are generally acknowledged [1], the first stages of the *in situ* genesis of gas embolism, as well as the immediately subsequent biophysical and biological processes lack comprehensive characterization. Critical phenomena associated with gas embolism, such as bubble nucleation within blood vessels, bloodstream supersaturation, endothelial injury, and inflammatory responses, have received limited attention in studies replicating physiological environments. Most *in vitro* studies have relied on basic two-dimensional microfluidic systems that overlooked the complicated flow of 3D blood vessels and lacked essential components like endothelial linings, real blood flow, coagulation, and oxygen gradients [18], [19], [20], [21], [22], [23]. These models are inherently limited in their power to predict gas embolism outcomes. On the other hand, *in-vivo* animal studies typically emphasized survival or systemic physiological responses, rather than underlying mechanisms at microscopic range [12], [13], [14], [15], [16], [17]. No current experimental platform connects controlled *in vitro* studies with physiologically relevant *in vivo* models to understand the dynamic progression of gas embolism, from bubble nucleation or gas entry to endothelial damage and systemic effects. This methodological and mechanistic gap has resulted in a fragmented, limited research focus, in particular on the life-threatening aspects of gas embolism.

Difficult diagnosis: The diagnosis of gas embolism is often delayed or missed due to rapid clinical progression, symptomatology overlapping with other acute conditions, the limited lifespan of gas emboli, and technological constraints in detecting intravascular gas [78]. Symptoms such as chest pain, respiratory compromise, hypotension, and neurologic deficits are often indistinguishable from those of acute stroke, myocardial infarction, or sepsis [6], [191]. This can lead to misdiagnosis, especially when classical risk factors like diving or cardiac surgery are absent. On the imaging side, chest radiography may occasionally reveal pulmonary embolism secondary to gas embolism as decreased pulmonary perfusion [192], but its sensitivity and specificity are poor, especially for small or moderate gas volumes [193]. The sensitivity of MRI is limited by its optimal imaging time, often requiring several to up to 24 hours for ischemic changes to become visible [191]. The sensitivity of CT for gas embolism is also reduced by the reabsorption of gas over time, poor visualization of microbubbles, and ambiguity in identifying low-density structures. Even with optimized protocols, CT may fail to detect or quantify emboli accurately [194]. Transcranial Doppler sonography is limited by inadequate resolution for small bubbles, calibration issues, and non-specific signal characteristics [195]. Although TEE offers high sensitivity for detecting intravascular gas in central circulation, it is semi-invasive, requires advanced clinical expertise [196], and cannot detect bubbles in the cerebral or peripheral microvasculature [197]. Furthermore, most diagnostic tools, with the possible exception of Doppler ultrasound, are expensive, non-portable, and unsuitable for real-time or systemic monitoring. The absence of portable or biomarker-based methods leaves diagnosis reliant on low clinical suspicion, leading to frequent underdiagnosis and delayed treatment.

Fragmented interventions, limited options: Therapeutic strategies for gas embolism are significantly narrow, with HBOT being broadly regarded as the most highly endorsed approach [190]. However, access to HBOT is often restricted outside major centers, owing to the relative scarcity of specialized equipment, trained clinicians, and timely patient transfer [198]. Even in advanced centers, delays can reduce efficacy, especially in cerebral or cardiopulmonary cases [199]. Although preclinical studies involving corticosteroids (for pulmonary gas embolism), [200], anticoagulants [97], membrane stabilizers [201], and anti-inflammatory agents [202] have shown promise, no pharmacological treatment for gas embolism has received regulatory approval. A better understanding of gas embolism pathogenesis and pathophysiology, as well as more comprehensive models for therapeutic validation could evaluate these potential treatment options. Preventive strategies, including air filtration [203], CO_2 flushing [204], patient positioning [205], and aspiration techniques [206], are inconsistently used and rarely follow standardized protocols.

Lacking priority, missing investment: Insufficient research investment in gas embolism has hindered scientific advancement, with minimal progress in mechanistic understanding or therapeutic innovation [8], [207]. Insufficient institutional prioritization and the absence of dedicated research infrastructure are key issues. Commercial interest is also limited due to the unpredictable incidence of gas embolism across patient populations, making investment in specialized solutions less appealing [208]. Its exclusion from major health agendas along with restricted research funding, low public health awareness, and inadequate surveillance efforts, forms a set of factors that collectively reinforce its marginalization within healthcare policy and funding structures [209].

B. Improving Prevention, Diagnostics, and Treatment

Global surveillance, education, and advocacy: The development of a comprehensive, standardized, multinational registry that systematically collects clinical and environmental data, together with standardized measurement protocols, could help to improve comprehension of gas embolism across diverse

contexts, from medical procedures to extreme environmental exposures. Retrospective analysis of existing datasets could help to provide a more holistic insight into incidence patterns and risk factors. Through recognizing complex, non-linear patterns in clinical data, artificial intelligence and machine learning techniques could help to refine analytical detail and predict performance [210]. A robust surveillance infrastructure could support the development of evidence-based guidelines, healthcare planning, and funding prioritization. Strategic collaboration with patient organizations, similar to the Divers Alert Network, the Trauma Survivors Network, and Lifebox, could raise awareness and reduce barriers to care. When linked with educational campaigns and patient-oriented research, these partnerships could facilitate community engagement and reinforce prevention efforts. The lack of knowledge regarding gas embolism in global health strategies and public awareness, alongside limited funding, requires advocacy to include it in priority lists of World Health Organization (WHO) and to ensure dedicated support from major funding organizations. The leadership of professional societies is crucial for creating evidence-based consensus guidelines and ensuring their consistent clinical adoption. Simultaneously, enhancing public engagement through social awareness and advocacy is needed, especially in cases linked to stigmatized causes.

Fundamentals-based prevention: A comprehensive understanding of gas embolism mechanisms, especially nucleation and distribution of bubbles, and subsequently endothelial damage, and inflammatory signaling would benefit from a bioengineered platform that accurately mimics anatomical and physiological features. Endothelialized 3D organ-on-chip systems [211] may be able to provide physiologically relevant environments to study emboli dynamics. Integrating biomimetic microvascular models with mini-hyperbaric chambers to simulate DCS may provide a more detailed mechanistic understanding of DCS in extreme exposure scenarios. Establishing a solid integrative framework between *in vivo*, *in vitro*, and *in silico* research on local and systemic gas embolism is needed to overcome the shortcomings of existing *in vitro* models. This connection supports the improvement and validation of these models to better reflect physiological and pathological processes.

Advanced diagnostics: Developing additional portable diagnostic tools for real-time visualization of intravascular bubbles is desirable. Integrating imaging approaches, like Doppler ultrasound, MRI, echocardiography, and photoacoustic imaging could enable more rapid and convenient detection during emergencies and surgeries. Incorporating artificial intelligence into imaging workflows and analyzing clinical data could enhance detection of subtle emboli on CT and MRI [210], [212]. Assessing circulating biomarkers might provide diagnostic support after bubble resolution. These diagnostic advances could improve outcomes, support epidemiological data collection, and address the longstanding neglect of gas embolism.

Diversification of therapeutic strategies: The constraints of HBOT access and its time-intensive nature highlight the necessity of prioritizing the development of supplementary therapeutic approaches. Administering pharmacological agents such as antioxidants, anti-inflammatory drugs, and endothelial protectants in combination with HBOT in suspected cases, if approved, may reduce secondary tissue damage and improve overall outcomes. Integrating artificial intelligence to continuously interpret diagnostic imaging and other physiological data in real time, while fine-tuning HBOT protocols, may improve treatment outcomes. The consistent application of standardized preventive interventions, incorporating refined surgical techniques, patient positioning protocols, automated intravenous air detection, and procedural safeguards, to decrease incidence may also be important. Developing diverse, accessible treatments could improve better outcomes and promote recognition of gas embolism as a significant clinical concern rather than a neglected condition.

V. Conclusion

Gas embolism exemplifies a complex disorder—potentially serious to lethal in nature, yet obscured by heterogeneous clinical documentation and insufficient epidemiological understanding. The pathogenesis of gas embolism arises from thermodynamic factors, yet its downstream trajectory is critically shaped by endothelial cell interactions with intravascular bubbles. Endothelial mechanical disruption from intravascular bubbles initiates clot formation; the resulting occlusive state sustains a feed-forward loop of inflammation and thrombus enlargement. In replicating gas embolism, *in vitro* and *in silico* models may provide useful platforms to complement *in vivo* studies and facilitate mechanistic exploration. Their limited anatomical fidelity, together with elements of cellular responses, can be mitigated in part through the incorporation of three-dimensional structures together with endothelial cell cultures. A major limitation in gas embolism diagnosis is the absence of universally accepted, reliable, and conveniently applied imaging techniques. Although TEE and CT demonstrate high context-dependent sensitivity, their application is constrained by temporal factors, patient stability, and procedural limitations. This limited diagnostic effectiveness undermines treatment outcomes. Early supportive interventions are important, with HBOT recognized as the most validated treatment strategy. Surfactant intervention could be an adjunctive pharmacological approach, targeting bubble-induced mechanical stress to lower endothelial inflammation and thereby protect vascular integrity. Despite its critical nature, gas embolism remains underappreciated due to inadequate surveillance, limited research support, insufficient clinical recognition, and shortcomings in diagnostic and therapeutic resources. Future advances in *in vitro* and *in silico* studies require coordinated global advocacy, robust registry infrastructures, innovative in-vitro modeling, portable diagnostic solutions, and expanded accessible treatment modalities beyond HBOT to address current clinical limitations.

Appendix

The supplementary materials are provided to support and illustrate key points discussed in the main text.

References

[1] S. Goldman et al., *Gas Bubble Dynamics in the Human Body*. New York, NY, USA: Academic, 2017.

[2] J. Wang et al., "Microbubble biointerfacing by regulation of the platelet membrane surfactant activity at the gas-liquid interface for acute thrombosis targeting," *Angewandte Chemie Int. Ed.*, vol. 63, no. 9, 2024, Art. no. e202314583.

[3] S. Gordy and S. Rowell, "Vascular air embolism," *Int. J. Crit. Illness Inj. Sci.*, vol. 3, no. 1, pp. 73–76, 2013.

[4] D. Ghosh et al., "Decompression illness-critical review," *J. Mar. Med. Soc.*, vol. 17, no. 1, pp. 20–29, 2015.

[5] D. Hatling et al., "Iatrogenic cerebral gas embolism–A systematic review of case reports," *Acta Anaesthesiologica Scandinavica*, vol. 63, no. 2, pp. 154–160, 2019.

[6] P. L. Marsh et al., "Iatrogenic air embolism: Pathoanatomy, thromboinflammation, endotheliopathy, and therapies," *Front. Immunol.*, vol. 14, 2023, Art. no. 1230049.

[7] I. J. R. Walker et al., *Diving Gas Embolism*. St. Petersburg, FL, USA: StatPearls Publishing, 2025.

[8] H. Alzghoul et al., "Venous air embolism: A systematic review," *Chest Crit. Care*, vol. 2, no. 1, 2024, Art. no. 100049.

[9] T. S. Neuman, "Arterial gas embolism and decompression sickness," *Physiology*, vol. 17, no. 2, pp. 77–81, 2002.

[10] M. M. Wilson and F. J. Curley, "Gas embolism: Part I. Venous gas emboli," *J. Intensive Care Med.*, vol. 11, no. 4, pp. 182–204, 1996.

[11] S. J. Mitchell et al., "Decompression sickness and arterial gas embolism," *New England J. Med.*, vol. 386, no. 13, pp. 1254–1264, 2022.

[12] C. C. Fries et al., "Experimental cerebral gas embolism," *Ann. Surg.*, vol. 145, no. 4, pp. 461–470, 1957.

[13] H. J. Geissler et al., "Cooling gradients and formation of gaseous microemboli with cardiopulmonary bypass: An echocardiographic study," *Ann. Thoracic Surg.*, vol. 64, no. 1, pp. 100–104, 1997.

[14] V. Palikov et al., "Effect of a helium and oxygen mixture on physiological parameters of rats with cerebral arterial air embolism," *Front. Physiol.*, vol. 15, 2024, Art. no. 1388331.

[15] H. Richardson et al., "Experimental gas embolism: I. Intravenous air embolism," *Can. Med. Assoc. J.*, vol. 36, no. 6, pp. 584–588, 1937.

[16] N. J. Robinson et al., "A baseline model for estimating the risk of gas embolism in sea turtles during routine dives," *Front. Physiol.*, vol. 12, 2021, Art. no. 678555.

[17] A. Velázquez-Wallraf et al., "Establishment of a fish model to study gas-bubble lesions," *Sci. Rep.*, vol. 12, no. 1, 2022, Art. no. 6592.

[18] K. Baassiri and D. V. Nicolau, "Understanding the impact of synthetic hematocrit levels and biomimetic channel widths on bubble parameters in vascular systems on a chip," *Biomimetics*, vol. 10, no. 2, 2025, Art. no. 98.

[19] D. Bento et al., "Bubbles moving in blood flow in a microchannel network: The effect on the local hematocrit," *Micromachines*, vol. 11, no. 4, 2020, Art. no. 344.

[20] D. Bento et al., "Blood flow of bubbles moving in microchannels with bifurcations," in *Proc. VII ECCOMAS Thematic Conf. Comput. Vis. Med. Image Process.*, 2019, pp. 571–577.

[21] Z. Li et al., "Flow field around bubbles on formation of air embolism in small vessels," *Proc. Nat. Acad. Sci.*, vol. 118, no. 26, 2021, Art. no. e2025406118.

[22] P. Ma et al., "An integrated microfluidic device for studying controllable gas embolism induced cellular responses," *Talanta*, vol. 208, 2020, Art. no. 120484.

[23] M. M. Mardanpour et al., "Investigation of air bubble behaviour after gas embolism events induced in a microfluidic network mimicking microvasculature," *Lab Chip*, vol. 24, no. 9, pp. 2518–2536, 2024.

[24] C. J. McCarthy et al., "Air embolism: Diagnosis, clinical management and outcomes," *Diagnostics*, vol. 7, no. 1, 2017, Art. no. 5.

[25] C. M. Muth and E. S. Shank, "Gas embolism," *New England J. Med.*, vol. 342, no. 7, pp. 476–482, 2000.

[26] D. Legendre and R. Zenit, "Gas bubble dynamics," *Rev. Modern Phys.*, vol. 97, no. 2, 2025, Art. no. 025001.

[27] S. Van Poucke et al., "The release of dissolved gases from solution during decompression after hyperbaric treatment: Effervescent tables and Henry's law," *Anesthesiology/Amer. Soc. Anesthesiologists.-Philadelphia*, vol. 95, no. 3, pp. 816–816, 2001.

[28] D. D. van Slyke, "The determination of gases and other solutions by vacuum extraction and manometric measurement: III. Gasometric determination of methemoglobin," *J. Biol. Chem.*, vol. 66, no. 2, pp. 409–414, 1925.

[29] D. E. Weitkamp and M. Katz, "A review of dissolved gas supersaturation literature," *Trans. Amer. Fisheries Soc.*, vol. 109, no. 6, pp. 659–702, 1980.

[30] M. Lechner et al., "Otorhinolaryngology and diving—Part 1: Otorhinolaryngological hazards related to compressed gas scuba diving: A review," *JAMA Otolaryngology–Head Neck Surg.*, vol. 144, no. 3, pp. 252–258, 2018.

[31] D. Knotts et al., "Pneumothorax volume expansion in helicopter emergency medical services transport," *Air Med. J.*, vol. 32, no. 3, pp. 138–143, 2013.

[32] R. Matthews et al., "043 A case of cerebral air embolism from giant pulmonary bulla during air travel," *J. Neurol., Neurosurgery Psychiatry*, vol. 93, no. 6, pp. A114–A114, 2022.

[33] S. S.-M. Wong et al., "Venous air embolism related to the use of central catheters revisited: With emphasis on dialysis catheters," *Clin. Kidney J.*, vol. 10, no. 6, pp. 797–803, 2017.

[34] A. A. Zikry et al., "Carbon dioxide embolism during laparoscopic sleeve gastrectomy," *J. Anaesthesiol., Clin. Pharmacol.*, vol. 27, no. 2, pp. 262–265, 2011.

[35] W. Kanjo et al., "Massive pulmonary embolism led to cardiac arrest two days after thoracoscopy in a young male with pleural tuberculosis," *Respirology Case Rep.*, vol. 11, no. 6, 2023, Art. no. e01069.

[36] A. Ghosh et al., "Intraoperative challenge: Managing venous air embolism during sitting craniotomy," *Cureus*, vol. 16, no. 6, 2024, Art. no. e61484.

[37] O. Rena et al., "Air-leak management after upper lobectomy in patients with fused fissure and chronic obstructive pulmonary disease: A pilot trial comparing sealant and standard treatment," *Interactive Cardiovasc. Thoracic Surg.*, vol. 9, no. 6, pp. 973–977, 2009.

[38] L. O. S. Suastika and Y. H. Oktaviono, "Multiple air embolism during coronary angiography: How do we deal with it?," *Clin. Med. Insights: Cardiol.*, vol. 10, pp. CMC–S38040, 2016.

[39] S. Balboa et al., "Position is important: Retrograde air embolism after central venous catheter removal," *Neurologia*, vol. 38, no. 3, pp. 223–225, 2023.

[40] V. Vukadinovic et al., "Clinical features of pulmonary emboli in patients following cytoreductive surgery (peritonectomy) and hyperthermic intraperitoneal chemotherapy (HIPEC), a single centre experience," *Eur. J. Surg. Oncol.*, vol. 41, no. 5, pp. 702–706, 2015.

[41] R. Arieli, "In vitro evidence of decompression bubble dynamics and gas exchange on the luminal aspect of blood vessels: Implications for size distribution of venous bubbles," *Physiol. Rep.*, vol. 7, no. 24, 2019, Art. no. e14317.

[42] E. Søfteland et al., "Nitrogen microbubbles induce a disappearance of single platelets (aggregation) with porcine platelets: A comparative study of the effects of anticoagulants and blood collection methods," *Thromb. Res.*, vol. 76, no. 1, pp. 61–70, 1994.

[43] E. Kliuchnikov et al., "Exploring effects of platelet contractility on the kinetics, thermodynamics, and mechanisms of fibrin clot contraction," *NPJ Biol. Phys. Mechan.*, vol. 2, no. 1, 2025, Art. no. 6.

[44] F. Swieringa et al., "Integrating platelet and coagulation activation in fibrin clot formation," *Res. Pract. Thromb. Haemostasis*, vol. 2, no. 3, pp. 450–460, 2018.

[45] A. O. Brubakk et al., "A single air dive reduces arterial endothelial function in man," *J. Physiol.*, vol. 566, no. 3, pp. 901–906, 2005.

[46] P. Sobolewski et al., "Air bubble contact with endothelial cells causes a calcium-independent loss in mitochondrial membrane potential," *Biophysical J.*, vol. 104, no. 2, pp. 215a–216a, 2013.

[47] C. Zhang, "The role of inflammatory cytokines in endothelial dysfunction," *Basic Res. Cardiol.*, vol. 103, pp. 398–406, 2008.

[48] M. Y. Najem et al., "Cytokine and chemokine regulation of venous thromboembolism," *J. Thromb. Haemostasis*, vol. 18, no. 5, pp. 1009–1019, 2020.

[49] N. Gupta et al., "The stimulation of thrombosis by hypoxia," *Thromb. Res.*, vol. 181, pp. 77–83, 2019.

[50] D. N. Granger and P. R. Kvietys, "Reperfusion injury and reactive oxygen species: The evolution of a concept," *Redox Biol.*, vol. 6, pp. 524–551, 2015.

[51] M. G. Scioli et al., "Oxidative stress and new pathogenetic mechanisms in endothelial dysfunction: Potential diagnostic biomarkers and therapeutic targets," *J. Clin. Med.*, vol. 9, no. 6, 2020, Art. no. 1995.

[52] S. J. Mitchell, "Decompression illness: A comprehensive overview," *Diving Hyperbaric Med.*, vol. 54, no. 1Suppl, pp. 1–53, 2024.

[53] S. R. Thom et al., "Microparticles initiate decompression-induced neutrophil activation and subsequent vascular injuries," *J. Appl. Physiol.*, vol. 110, no. 2, pp. 340–351, 2011.

[54] R. D. Vann et al., "Decompression illness," *Lancet*, vol. 377, no. 9760, pp. 153–164, 2011.

[55] W. G. Malette et al., "Dysbarism. A review of thirty-five cases with suggestion for therapy," *Aerosp. Med.*, vol. 33, pp. 1132–1139, 1962.

[56] F. Brunner et al., "Post-decompression shock due to extravasation of plasma," *Lancet*, vol. 1, pp. 1071–1073, 1964.

[57] V. Nossum et al., "Endothelial damage by bubbles in the pulmonary artery of the pig," *Undersea Hyperbaric Med.*, vol. 26, no. 1, pp. 1–8, 1999.

[58] V. Nossum et al., "Small amounts of venous gas embolism cause delayed impairment of endothelial function and increase polymorphonuclear neutrophil infiltration," *Eur. J. Appl. Physiol.*, vol. 86, pp. 209–214, 2002.

[59] L. L. Levin et al., "Blood and blood vessel wall changes induced by decompression sickness in dogs," *J. Appl. Physiol.*, vol. 50, pp. 944–949, 1981.

[60] S. C. Helps et al., "Increasing doses of intracarotid air and cerebral blood flow in rabbits," *Stroke*, vol. 21, pp. 1340–1345, 1990.

[61] S. C. Helps and D. F. Gorman, "Air embolism of the brain in rabbits pre-treated with mechlorethamine," *Stroke*, vol. 22, pp. 351–354, 1991.

[62] N. B. Hampson and R. E. Moon, "Arterial gas embolism breathing compressed air in 1.2 metres of water," *Diving Hyperbaric Med.*, vol. 50, no. 3, pp. 292–294, 2020.

[63] U. Lindblom and C. Tosterud, "Pulmonary barotrauma with cerebral arterial gas embolism from a depth of 0.75-1.2 metres of fresh water or less: A case report," *Diving Hyperbaric Med.*, vol. 51, no. 2, pp. 224–226, 2021.

[64] K. Tetzlaff et al., "Hyperbaric chamber-related decompression illness in a patient with asymptomatic pulmonary sarcoidosis," *Aviation, Space, Environ. Med.*, vol. 70, no. 6, pp. 594–597, 1999.

[65] D. K. Buschmann, "Arterial gas embolism during pressure tolerance testing in a hyperbaric chamber: A report of two cases," *Aviation, Space, Environ. Med.*, vol. 81, no. 12, pp. 1133–1136, 2010.

[66] H. K. Wolf et al., "Barotrauma and air embolism in hyperbaric oxygen therapy," *Amer. J. Forensic Med. Pathol.*, vol. 11, pp. 149–153, 1990.

[67] S. Jung et al., "Cerebral air embolism caused by a bronchogenic cyst," *Practical Neurol.*, vol. 10, no. 3, pp. 164–166, 2010.

[68] S. L. Zhao et al., "Gas embolism after hydrogen peroxide use during spine surgery: Case report and literature review," *World Neurosurgery*, vol. 143, pp. 228–231, 2020.

[69] A. King et al., "Timing of embolic phenomena after hydrogen peroxide exposure - A systematic review," *Clin. Toxicol.*, vol. 61, no. 1, pp. 12–21, 2023.

[70] C. V. Zwirewich et al., "Noncardiogenic pulmonary edema caused by decompression sickness: Rapid resolution following hyperbaric therapy," *Radiology*, vol. 163, pp. 81–82, 1987.

[71] D. M. Frim et al., "Acute pulmonary edema after low-level air embolism during craniotomy. Case report," *J. Neurosurgery*, vol. 85, no. 5, pp. 937–940, 1996.

[72] S. Wood and G. Fuzaylov, "Acute pulmonary edema due to occult air embolism detected on an automated anesthesia record: Illustrative case," *J. Neurosurgery: Case Lessons*, vol. 1, no. 3, 2021, Art. no. CASE2075.

[73] B. D. Butler and B. A. Hills, "Transpulmonary passage of venous air emboli," *J. Appl. Physiol.*, vol. 59, pp. 543–547, 1985.

[74] A. Vik et al., "Venous air embolism in swine: Transport of gas bubbles through the pulmonary circulation," *J. Appl. Physiol.*, vol. 69, no. 1, pp. 237–244, 1990.

[75] A. Vik et al., "Effect of aminophylline on transpulmonary passage of venous air emboli in pigs," *J. Appl. Physiol.*, vol. 71, no. 5, pp. 1780–1786, 1991.

[76] M. W. Eldridge et al., "Exercise-induced intrapulmonary arteriovenous shunting in healthy humans," *J. Appl. Physiol.*, vol. 97, no. 3, pp. 797–805, Sep. 2004.

[77] R. E. Moon and S. J. Mitchell, "Hyperbaric treatment of air or gas embolism: Current recommendations," *Undersea Hyperbaric Med.*, vol. 52, no. 1, pp. 41–53, 2025.

[78] T. Edwards et al., "Abnormal exercise gas exchange before pulmonary emboli diagnosis," *Mayo Clinic Proc.: Innov., Qual. Outcomes*, vol. 8, no. 6, pp. 530–535, 2024.

[79] M. R. Dardeau et al., "The incidence of decompression illness in 10 years of scientific diving," *Diving Hyperbaric Med.*, vol. 42, no. 4, pp. 195–200, 2012.

[80] R. G. Dunford et al., "A study of decompression sickness using recorded depth-time profiles," *Undersea Hyperbaric Med.*, vol. 47, no. 1, 2020.

[81] J. Bessereau et al., "Long-term outcome of iatrogenic gas embolism," *Intensive Care Med.*, vol. 36, no. 7, pp. 1180–1187, 2010.

[82] M. C. Freund et al., "Systemic air embolism during percutaneous core needle biopsy of the lung: Frequency and risk factors," *BMC Pulmonary Med.*, vol. 12, no. 1, 2012, Art. no. 2.

[83] P. Mandelstam et al., "Complications associated with esophagogastroduodenoscopy and with esophageal dilation," *Gastrointestinal Endoscopy*, vol. 23, no. 1, pp. 16–19, 1976.

[84] A. Verma and M. P. Singh, "Venous gas embolism in operative hysteroscopy: A devastating complication in a relatively simple surgery," *J. Anaesthesiol. Clin. Pharmacol.*, vol. 34, no. 1, pp. 103–106, 2018.

[85] S. Fuentes et al., "Gas embolism in pediatric minimally invasive surgery: Should it be a concern?," *J. Laparoendoscopic Adv. Surg. Techn.*, vol. 33, no. 10, pp. 1011–1017, 2023.

[86] R. Dunford et al., "The incidence of venous gas emboli in recreational diving," *Undersea Hyperbaric Med.*, vol. 29, no. 4, pp. 247–259, 2002.

[87] S. L. Blogg et al., "Agreement of precordial and subclavian Doppler ultrasound venous gas emboli grades in a large diving data set," *Diving Hyperbaric Med.*, vol. 55, no. 1, pp. 2–10, 2025.

[88] A. Jasudavisius et al., "A systematic review of transthoracic and transesophageal echocardiography in non-cardiac surgery: Implications for point-of-care ultrasound education in the operating room," *Can. J. Anesth./J. Canadien d'anesthésie*, vol. 63, no. 4, pp. 480–487, 2016.

[89] E. M. Chung et al., "Size distribution of air bubbles entering the brain during cardiac surgery," *PLoS One*, vol. 10, no. 4, 2015, Art. no. e0122166.

[90] J. Benson et al., "Hyperbaric oxygen therapy of iatrogenic cerebral arterial gas embolism," *Undersea Hyperbaric Med.*, vol. 30, no. 2, pp. 117–126, 2003.

[91] R. A. van Hulst et al., "Gas embolism: Pathophysiology and treatment," *Clin. Physiol. Funct. Imag.*, vol. 23, no. 5, pp. 237–246, 2003.

[92] T. Yu et al., "Branch-like gas in a commercial diver's liver: A case report," *Undersea Hyperbaric Med.*, vol. 47, no. 2, pp. 267–270, 2020.

[93] T. C. Schaefer et al., "Iatrogenic air embolism: Influence of air bubble size on cerebral infarctions in an experimental in vivo and numerical simulation model," *J. NeuroInterventional Surg.*, vol. 16, no. 10, pp. 1036–1041, 2024.

[94] S. Mitchell, "Lidocaine in the treatment of decompression illness: A review of the literature," *Undersea Hyperbaric Med.*, vol. 28, no. 3, pp. 165–174, 2001.

[95] R. Moon, "Hyperbaric oxygen treatment for air or gas embolism," *Undersea Hyperbaric Med.*, vol. 41, no. 2, pp. 159–166, 2014.

[96] T. M. Vesely, "Air embolism during insertion of central venous catheters," *J. Vasc. Interventional Radiol.*, vol. 12, no. 11, pp. 1291–1295, 2001.

[97] N. Shaikh and F. Ummunisa, "Acute management of vascular air embolism," *J. Emergencies, Trauma, Shock*, vol. 2, no. 3, pp. 180–185, 2009.

[98] J. Bazin et al., "Haemodynamic conditions enhancing gas embolism after venous injury during laparoscopy: A study in pigs," *Brit. J. Anaesth.*, vol. 78, no. 5, pp. 570–575, 1997.

[99] S. J. Brull and R. C. Prielipp, "Vascular air embolism: A silent hazard to patient safety," *J. Crit. Care*, vol. 42, pp. 255–263, 2017.

[100] C. Ross et al., "Acute management of high-risk and intermediate-risk pulmonary embolism in children: A review," *Chest*, vol. 161, no. 3, pp. 791–802, 2022.

[101] P.-M. Roy et al., "Contemporary management of acute pulmonary embolism," *Trends Cardiovasc. Med.*, vol. 32, no. 5, pp. 259–268, 2022.

[102] Z. Chen et al., "Artificial vascular with pressure-responsive property based on deformable microfluidic channels," *Adv. Healthcare Mater.*, vol. 13, no. 20, 2024, Art. no. 2304532.

[103] R. Ariati et al., "Polydimethylsiloxane composites characterization and its applications: A review," *Polymers*, vol. 13, no. 23, 2021, Art. no. 4258.

[104] C. Leguy et al., "Estimation of distributed arterial mechanical properties using a wave propagation model in a reverse way," *Med. Eng. Phys.*, vol. 32, no. 9, pp. 957–967, 2010.

[105] I. Ramos et al., "PDMS surface wettability modification and its applications: A systematic review," *J. Mol. Liquids*, 2025, Art. no. 127978.

[106] H.-H. Weitkemper et al., "Gaseous microemboli and the influence of microporous membrane oxygenators," *J. ExtraCorporeal Technol.*, vol. 37, no. 3, pp. 256–264, 2005.

[107] M. Puthettu et al., "Effect of cannulation site on emboli travel during cardiac surgery," *J. Cardiothoracic Surg.*, vol. 16, no. 1, 2021, Art. no. 181.

[108] A. J. Calderón et al., "Microfluidic model of bubble lodging in microvessel bifurcations," *Appl. Phys. Lett.*, vol. 89, no. 24, 2006.

[109] E. Nader et al., "Blood rheology: Key parameters, impact on blood flow, role in sickle cell disease and effects of exercise," *Front. Physiol.*, vol. 10, 2019, Art. no. 1329.

[110] V. Papadopoulou et al., "A critical review of physiological bubble formation in hyperbaric decompression," *Adv. Colloid Interface Sci.*, vol. 191, pp. 22–30, 2013.

[111] M. Barak and Y. Katz, "Microbubbles," *Chest*, vol. 128, no. 4, pp. 2918–2932, 2005.
[112] J. A. Leo et al., "Shear-thinning behaviour of blood in response to active hyperaemia: Implications for the assessment of arterial shear stress-mediated dilatation," *Exp. Physiol.*, vol. 105, no. 2, pp. 244–257, 2020.
[113] M. Habibi Matin and S. Moghaddam, "On the extension of Bretherton theory for thin liquid films formed around elongated bubbles," *Phys. Fluids*, vol. 33, no. 12, 2021.
[114] F. P. Bretherton, "The motion of long bubbles in tubes," *J. Fluid Mechan.*, vol. 10, pp. 166–188, 1961.
[115] A. Fuchs et al., "Assessment of rheological models applied to blood flow in human thoracic aorta," *Bioengineering*, vol. 10, no. 11, 2023, Art. no. 1240.
[116] K. Mukundakrishnan et al., "Bubble motion in a blood vessel: Shear stress induced endothelial cell injury," *J. Biomechanical Eng.*, vol. 131, no. 7, 2009, Art. no. 745161.
[117] K. Mukundakrishnan et al., "Numerical study of wall effects on buoyant gas-bubble rise in a liquid-filled finite cylinder," *Phys. Rev. E—Stat., Nonlinear, Soft Matter Phys.*, vol. 76, no. 3 Pt 2, 2007, Art. no. 036308.
[118] D. M. Eckmann et al., "Hydrodynamics and interfacial surfactant transport in vascular gas embolism," *J. Heat Transfer*, vol. 143, no. 10, 2021, Art. no. 100802.
[119] K. Mukundakrishnan et al., "Drop motion through a Carreau-Yasuda fluid flowing in a vertical tube," in *Proc., ISHMT-ASME Heat Mass Transfer*, 2008, pp. US–11–1–US–11–8.
[120] K. Mukundakrishnan et al., "Bubble motion through a generalized power-law fluid flowing in a vertical tube," *Ann. New York, NY, USA Acad. Sci.*, vol. 1161, pp. 256–267, 2009.
[121] T. N. Swaminathan et al., "Surfactant properties differentially influence intravascular gas embolism mechanics," *Ann. Biomed. Eng.*, vol. 38, no. 12, pp. 3649–3663, 2010.
[122] T. N. Swaminathan et al., "Effect of a soluble surfactant on a finite sized bubble motion in a blood vessel," *J. Fluid Mechan.*, vol. 642, pp. 509–539, 2010.
[123] J. Zhang et al., "A front tracking method for a deformable intravascular axisymmetric bubble with a soluble surfactant," *J. Comput. Phys.*, vol. 214, pp. 366–396, 2006.
[124] K. Mukundakrishnan et al., "Computational simulation of hematocrit effects on arterial gas embolism dynamics," *Aviation, Space, Environ. Med.*, vol. 83, no. 2, pp. 92–101, Feb. 2012.
[125] C. W. Park, "Influence of soluble surfactants on the motion of a finite bubble in a capillary-tube," *Phys. Fluids a-Fluid*, vol. 4, no. 11, pp. 2335–2347, Nov. 1992.
[126] A. L. Moloff, "Delayed onset arterial gas embolism," *Aviation, Space, Environ. Med.*, vol. 64, no. 11, pp. 1040–1043, 1993.
[127] S. E. Harvey et al., "Delayed-onset arterial gas embolism after underwater egress training," *Aerosp. Med. Hum. Perform.*, vol. 95, no. 11, pp. 867–870, 2024.
[128] G. J. Brooks et al., "Pulmonary barotrauma in submarine escape trainees and the treatment of cerebral arterial air embolism," *Aviation, Space, Environ. Med.*, vol. 57, no. 12 Pt 1, pp. 1201–1207, 1986.
[129] T. S. Neuman and A. A. Bove, "Combined arterial gas embolism and decompression sickness following no-stop dives," *Undersea Biomed. Res.*, vol. 17, pp. 429–436, 1990.
[130] R. R. Pearson and R. F. Goad, "Delayed cerebral edema complicating cerebral arterial gas embolism: Case histories," *Undersea Biomed. Res.*, vol. 9, pp. 283–296, 1982.
[131] R. A. Fakkert et al., "Computer tomography perfusion patterns in iatrogenic cerebral arterial gas embolism: A retrospective cohort study," *Eur. J. Radiol.*, vol. 170, 2024, Art. no. 111242.
[132] J. L. Guo et al., "Transesophageal echocardiography detection of air embolism during endoscopic surgery and validity of hyperbaric oxygen therapy: Case report," *Medicine*, vol. 100, no. 23, 2021, Art. no. e26304.
[133] K. Kandori et al., "Massive systemic arterial air embolism caused by an air shunt after blunt chest trauma: A case report," *Int. J. Surg. Case Rep.*, vol. 51, pp. 368–371, 2018.
[134] C. Yang et al., "Delayed presentation of air embolism within cerebral arteries following computed tomography-guided lung biopsy," *Cureus*, vol. 15, no. 1, 2023, Art. no. e33205.
[135] A. F. Caulfield et al., "MRI characteristics of cerebral air embolism from a venous source," *Neurology*, vol. 66, no. 6, pp. 945–946, 2006.
[136] Y. Hwang and Y. J. Kim, "Retrograde cerebral venous air embolism on susceptibility-weighted imaging," *Can. J. Neurological Sci.*, vol. 45, no. 4, pp. 464–465, 2018.
[137] S. C. Palmon et al., "Venous air embolism: A review," *J. Clin. Anesth.*, vol. 9, no. 3, pp. 251–257, 1997.
[138] T. M. Durant et al., "Pulmonary (venous) air embolism," *Amer. Heart J.*, vol. 33, pp. 269–281, 1947.
[139] P. Blanc et al., "Iatrogenic cerebral air embolism: Importance of an early hyperbaric oxygenation," *Intensive Care Med.*, vol. 28, no. 5, pp. 559–563, 2002.
[140] R. A. Fakkert et al., "Early hyperbaric oxygen therapy is associated with favorable outcome in patients with iatrogenic cerebral arterial gas embolism: Systematic review and individual patient data meta-analysis of observational studies," *Crit. Care*, vol. 27, no. 1, 2023, Art. no. 282.
[141] D. R. Leitch et al., "Cerebral arterial air embolism: I. Is there benefit in beginning HBO treatment at 6 bar?," *Undersea Biomed. Res.*, vol. 11, pp. 221–235, 1984.
[142] J. J. McDermott et al., "Comparison of two recompression profiles in treating experimental cerebral air embolism," *Undersea Biomed. Res.*, vol. 19, pp. 171–185, 1992.
[143] B. Zhang et al., "A comparison of the treatment outcomes of cerebral gas embolism at 2.8 ATA in comparison with 6 ATA," *Undersea Hyperbaric Med.*, vol. 51, no. 4, pp. 341–346, 2024.
[144] W. R. Johnson et al., "Comparison of treatment recompression tables for neurologic decompression illness in swine model," *PLoS One*, vol. 17, no. 10, 2022, Art. no. e0266236.
[145] B. Simonnet et al., "Therapeutic management of severe spinal cord decompression sickness in a hyperbaric center," *Front. Med.*, vol. 10, 2023, Art. no. 1172646.
[146] Navy Department, *U.S. Navy Diving Manual, Rev. 7, Change A, vol. 5, NAVSEA 0910-LP-115-1921*. Washington, DC, USA: Naval Sea Systems Command, Apr. 2018. [Online]. Available: https://www.navsea.navy.mil/Portals/103/Documents/SUPSALV/Diving/Dive%20Manual%20Rev%207%20Change%20A.pdf
[147] O. J. O'Neill et al., "The effect of total compression time and rate (slope) of compression on the incidence of symptomatic Eustachian tube dysfunction and middle ear barotrauma: A Phase II prospective study," *Undersea Hyperbaric Med.*, vol. 48, no. 3, 2021.
[148] S. Sherlock et al., "Audit of practice in Australasian hyperbaric units on the incidence of central nervous system oxygen toxicity," *Diving Hyperbaric Med.*, vol. 48, no. 2, pp. 73–78, 2018.
[149] S. Bonnington et al., "Oxygen toxicity seizures during United States navy treatment table 6: An acceptable risk in monoplace chambers?," *Diving Hyperbaric Med.*, vol. 51, no. 2, pp. 167–172, 2021.
[150] V. Mago, "Safety of hyperbaric medicine in clinical scenarios," *Ann. Afr. Med.*, vol. 23, no. 1, pp. 1–4, 2024.
[151] R. Whalen et al., "Cardiovascular and blood gas responses to hyperbaric oxygenation," *Amer. J. Cardiol.*, vol. 15, pp. 638–646, 1965.
[152] W. J. Whalen and P. Nair, "Skeletal muscle PO2: Effect of inhaled and topically applied O_2 and CO_2," *Amer. J. Physiol.-Legacy Content*, vol. 218, no. 4, pp. 973–980, 1970.
[153] T. C. Northfield, "Oxygen therapy for spontaneous pneumothorax," *Brit. Med. J.*, vol. 4, no. 5779, pp. 86–88, 1971.
[154] K. Nishina et al., "Intravenous lidocaine attenuates acute lung injury induced by hydrochloric acid aspiration in rabbits," *Anesthesiology*, vol. 88, pp. 1300–1309, 1998.
[155] D. S. Warner et al., "Insulin-induced normoglycemia improves ischemic outcome in hyperglycemic rats," *Stroke*, vol. 23, no. 12, pp. 1775–1780, 1992.
[156] K. H. Ryu et al., "Heparin reduces neurological impairment after cerebral arterial air embolism in the rabbit," *Stroke*, vol. 27, no. 2, pp. 303–309, 1996.
[157] J. M. Pontier et al., "Pharmacological intervention against bubble-induced platelet aggregation in a rat model of decompression sickness," *J. Appl. Physiol.*, vol. 110, no. 3, pp. 724–729, 2011.
[158] R. B. Philp et al., "Interactions between gas bubbles and components of the blood: Implications in decompression sickness," *Aerosp. Med.*, vol. 43, no. 9, pp. 946–953, 1972.
[159] B. A. Warren et al., "The ultrastructural morphology of air embolism: Platelet adhesion to the interface and endothelial damage," *Brit. J. Exp. Pathol.*, vol. 54, pp. 163–172, 1973.
[160] S. Manoharan et al., "Computational modeling of adiabatic bubble growth dynamics from submerged capillary-tube orifices in aqueous solutions of surfactants," *J. Heat Transfer*, vol. 141, no. 5, 2019, Art. no. 052002.
[161] S. Manoharan et al., "Visualization of multiscale processes - Bubble dynamics in surface active colloids," *J. Heat Transfer*, vol. 137, no. 8, 2015, Art. no. 080912.
[162] B. Eiseman et al., "Surface tension reducing substances in the management of coronary air embolism," *Ann. Surg.*, vol. 149, pp. 374–380, 1959.

[163] D. M. Eckmann and S. L. Diamond, "Surfactants attenuate gas embolism-induced thrombin production," *Anesthesiology*, vol. 100, no. 1, pp. 77–84, 2004.

[164] D. M. Eckmann et al., "Surfactant reduces platelet-bubble and platelet-platelet binding induced by *in vitro* air embolism," *Anesthesiology*, vol. 103, pp. 1204–1210, 2005.

[165] D. M. Eckmann et al., "Dose response of surfactants to attenuate gas embolism related platelet aggregation," *Heat Mass Transfer*, vol. 50, pp. 323–331, 2014.

[166] B. D. Spiess et al., "Protection from venous air embolism with fluorocarbon emulsion FC-43," *J. Surg. Res.*, vol. 41, no. 4, pp. 439–444, 1986.

[167] L. N. Torres et al., "Effects of perfluorocarbon emulsions on microvascular blood flow and oxygen transport in a model of severe arterial gas embolism," *J. Surg. Res.*, vol. 187, no. 1, pp. 324–333, 2014.

[168] D. A. Ingram et al., "Activation of complement by Fluosol attributable to the pluronic detergent micelle structure," *J. Cardiovasc. Pharmacol.*, vol. 22, no. 3, pp. 456–461, 1993.

[169] J. C. Briceno et al., "Oxygen transport and consumption during experimental cardiopulmonary bypass using oxyfluor," *ASAIO J.*, vol. 45, no. 4, pp. 322–327, 1999.

[170] B. Breyer et al., "The latent emulsifying capacity of human serum," *Clinica Chimica Acta*, vol. 11, no. 6, pp. 557–560, 1965.

[171] N. U. Khaliq et al., "Pluronic F-68 and F-127 based nanomedicines for advancing combination cancer therapy," *Pharmaceutics*, vol. 15, no. 8, 2023, Art. no. 2102.

[172] S. Kobayashi et al., "Microembolism bubble contact and calcium signaling in bovine aortic endothelial cells in vitro," *Undersea Hyperbaric Med.*, vol. 38, no. 1, pp. 27–39, 2011.

[173] P. Sobolewski et al., "Air bubble contact with endothelial cells in vitro induces calcium influx and IP3-dependent release of calcium stores," *Amer. J. Physiol.-Cell Physiol.*, vol. 301, no. 3, pp. C679–C686, 2011.

[174] C.-M. Chan et al., "Reactive oxygen species-dependent mitochondrial dynamics and autophagy confer protective effects in retinal pigment epithelial cells against sodium iodate-induced cell death," *J. Biomed. Sci.*, vol. 26, no. 1, 2019, Art. no. 40.

[175] A. L. Klinger et al., "Mechanotransductional basis of endothelial cell response to intravascular bubble contact," *Integrative Biol.*, vol. 3, pp. 1033–1042, 2011.

[176] A. L. Klinger et al., "Perfluorocarbon inhibition of bubble induced Ca^{2+} transients in an *in-vitro* model of vascular gas embolism," *Exp. Biol. Med.*, vol. 239, pp. 116–122, 2014.

[177] A. Suzuki and D. M. Eckmann, "Embolism bubble adhesion force in excised perfused microvessels," *Anesthesiology*, vol. 99, pp. 400–408, 2003.

[178] D. M. Eckmann and V. N. Lomivorotov, "Microvascular gas embolization clearance following perfluorocarbon administration," *J. Appl. Physiol.*, vol. 94, pp. 860–868, 2003.

[179] D. M. Eckmann and S. C. Armstead, "Surfactant reduction of cerebral infarct size and behavioral deficit in a rat model of cerebrovascular air embolism," *J. Appl. Physiol.*, vol. 115, pp. 868–876, 2013.

[180] K. Mukundakrishnan et al., "Finite-sized gas bubble motion in a blood vessel: Non-Newtonian effects," *Phys. Rev. E—Stat., Nonlinear, Soft Matter Phys.*, vol. 78, no. 3, 2008, Art. no. 036303.

[181] G. Berlot et al., "Uncommon occurrences of air embolism: Description of cases and review of the literature," *Case Rep. Crit. Care*, vol. 2018, no. 1, 2018, Art. no. 5808390.

[182] D. Y. Chuang et al., "Accidental air embolism: An uncommon cause of iatrogenic stroke," *Stroke*, vol. 50, no. 7, pp. e183–e186, 2019.

[183] T. A. Waheed et al., "Air embolism and st elevation myocardial infarction: A systematic review," *Circulation*, vol. 142, no. Suppl_3, 2020, Art. no. A14896.

[184] F. Clayton, "Iatrogenic air embolism complicating a case of severe septic shock," *Chest*, vol. 144, no. 4, 2013, Art. no. 300A.

[185] P. B. James, "Indications for oxygen therapy and the undersea and hyperbaric medical society," *Med. Gas Res.*, vol. 13, no. 4, p. 219, 2023.

[186] P. Buzzacott and P. Denoble, *DAN Annual Diving Report 2018 Edition: A Report on 2016 Diving Fatalities, Injuries, and Incidents*, Durham, England: Divers Alert Network, 2018, pp. 1–112.

[187] V. Červeňák et al., "Cerebral air embolism: Neurologic manifestations, prognosis, and outcome," *Front. Neurol.*, vol. 15, 2024, Art. no. 1417006.

[188] J. G. Jang et al., "A case of nonthrombotic pulmonary embolism after facial injection of hyaluronic acid in an illegal cosmetic procedure," *Tuberculosis Respir. Dis.*, vol. 77, no. 2, pp. 90–93, 2014.

[189] M. Szlaszynska et al., "Venous thromboembolism and chronic venous disease among people who inject drugs: A systematic review and meta-analysis," *Thromb. Update*, vol. 12, 2023, Art. no. 100141.

[190] M. Mirski et al., "Diagnosis and treatment of vascular air embolism," *Anesthesiology*, vol. 106, no. 1, pp. 164–215, 2007.

[191] P. Bothma and E. Lams, "Air or gas embolism," in *Encyclopedia of Forensic and Legal Medicine*, 3rd ed., J. Payne-James and R. W. Byard Eds. Amsterdam, The Netherlands: Elsevier, 2025, pp. 128–135.

[192] Y. Liu et al., "Chest X-ray feature of venous air embolism in orthopedic surgery in prone position: A case report," *Front. Surg.*, vol. 9, 2023, Art. no. 994839.

[193] R. H. Greenspan et al., "Accuracy of the chest radiograph in diagnosis of pulmonary embolism," *Invest. Radiol.*, vol. 17, no. 6, pp. 539–543, 1982.

[194] C. Brito et al., "Cerebral air embolism: The importance of computed tomography evaluation," *J. Med. Cases*, vol. 11, no. 12, p. 394–399, 2020.

[195] P. D. Hill, "The challenge of characterizing emboli by transcranial Doppler sonography," *Stroke*, vol. 25, no. 9, pp. 1882–1883, 1994.

[196] A. R. Nishant and M. M. Maddali, "Intraoperative transesophageal echocardiography: A sensitive and reliable tool for detecting air embolism in real time," *J. Cardiothoracic Vasc. Anesth.*, vol. 33, no. 3, pp. 878–880, 2019.

[197] T. R. Rau et al., "Automatic detection of venous air embolism using transesophageal echocardiography in patients undergoing neurological surgery in the semi-sitting position: A pilot study," *J. Clin. Monit. Comput.*, vol. 35, pp. 1103–1109, 2021.

[198] E. J. Thomas et al., "Case Report: Management of cerebral arterial gas embolism via transfer to an outpatient hyperbaric chamber," *Front. Med.*, vol. 12, 2025, Art. no. 1533459.

[199] S. A. Sokolowski et al., "Delayed treatment for decompression illness: Factors associated with long treatment delays and treatment outcome," *Diving Hyperbaric Med.*, vol. 52, no. 4, pp. 271–276, 2022.

[200] M. M. Sneeboer et al., "Oral and inhaled corticosteroid use and risk of recurrent pulmonary embolism," *Thromb. Res.*, vol. 140, pp. 46–50, 2016.

[201] D. E. Evans et al., "Effect of lidocaine after experimental cerebral ischemia induced by air embolism," *J. Neurosurgery*, vol. 70, no. 1, pp. 97–102, 1989.

[202] C.-C. Lan et al., "Surfactant attenuates air embolism-induced lung injury by suppressing NKCC1 expression and NF-κB activation," *Inflammation*, vol. 44, pp. 57–67, 2021.

[203] S. Lee and K. R. Bulsara, "Assessing the efficacy of commercially available filters in removing air micro-emboli in intravenous infusion systems," *J. ExtraCorporeal Technol.*, vol. 52, no. 2, pp. 118–125, 2020.

[204] T. Kölbel et al., "Carbon dioxide flushing technique to prevent cerebral arterial air embolism and stroke during TEVAR," *J. Endovascular Ther.*, vol. 23, no. 2, pp. 393–395, 2016.

[205] C. J. McCarthy et al., "Air embolism: Practical tips for prevention and treatment," *J. Clin. Med.*, vol. 5, no. 11, 2016, Art. no. 93.

[206] V. M. Daliparty et al., "Therapeutic manual aspiration of large venous air embolism in a patient with shock," *Chest*, vol. 162, no. 4, 2022, Art. no. A2093.

[207] R. Haldar and S. S. Bajwa, "Potential neuroendoscopic complications: An anesthesiologist's perspective," *Asian J. Neurosurgery*, vol. 14, no. 3, pp. 621–625, 2019.

[208] J. K. Stoller, "The challenge of rare diseases," *Chest*, vol. 153, no. 6, pp. 1309–1314, 2018.

[209] G. Baynam et al., "Global health for rare diseases through primary care," *Lancet Glob. Health*, vol. 12, no. 7, pp. e1192–e1199, 2024.

[210] A. Azarang et al., "Deep learning-based venous gas emboli grade classification in doppler ultrasound audio recordings," *IEEE Trans. Biomed. Eng.*, vol. 70, no. 5, pp. 1436–1446, May 2023.

[211] T. Yue et al., "A modular microfluidic system based on a multilayered configuration to generate large-scale perfusable microvascular networks," *Microsyst. Nanoeng.*, vol. 7, no. 1, 2021, Art. no. 4.

[212] H. Su et al., "A new machine learning model for predicting severity prognosis in patients with pulmonary embolism: Study protocol from Wenzhou, China," *Front. Neuroinform.*, vol. 16, 2022, Art. no. 1052868.